Layered nanoarchitectonics for condensed hard matter, soft matter, and living matter

Katsuhiko Ariga[1,2]

[1] Research Center for Materials Nanoarchitectonics, National Institute for Materials Science (NIMS), 1-1 Namiki, Tsukuba 305-0044, Japan.
[2] Graduate School of Frontier Sciences, The University of Tokyo, 5-1-5 Kashiwa-no-ha Kashiwa 277-8561, Japan.

E-mail: ARIGA.Katsuhiko@nims.go.jp

Received xxxxxx
Accepted for publication xxxxxx
Published xxxxxx

Abstract

Nanotechnology has elucidated scientific phenomena of various materials at the nano-level. The next step in materials developments is to build up materials, especially condensed matter, based on such nanotechnology-based knowledge. Nanoarchitectonics can be regarded as a post-nanotechnology concept. In nanoarchitectonics, functional material systems are architected from nanounits. Here, this review would like to focus on layered structures in terms of structure formation. The unit structures of layered structures are mostly two-dimensional materials or thin-film materials. They are attractive materials that have attracted much attention in modern condensed matter science. By organizing them into layered structures, we can expect to develop functions based on communication between the layers. Building up layered functional structures by assembling nano-layers of units is a typical approach in nanoarchitectonics. The discussion will be divided into the following categories: hard matter, hybrid, soft matter, and living object. For each target, several recent research examples will be given to illustrate the discussion. This paper will extract what aspects are considered important in the creation of the layered structure of each component. Layering strategies need to be adapted to the characteristics of the components. The type of structural precision and functionality required is highly dependent on the flexibility and mobility of the component. Furthermore, what is needed to develop the nanoarchitectonics of layered structures is discussedas future perspectives.

Keywords: nanoarchitectonics, layered material, hard matter, hybrid, soft matter, living object

1. Introduction

It can be said that the level of human life is determined by the materials available and the tools that can be processed from them. Material substances were originally extracted from nature in ancient days. However, various chemical and material science knowledge and technologies create artificial materials after scientific revolution. The history of mankind has been accompanied by the development of the science and technology of such materials, condensed matter. The importance of the science of producing materials is still recognized today, and functional materials are produced by organic chemistry [1-4], inorganic chemistry [5-8], coordination chemistry [9-12], polymer chemistry [13-16], supramolecular chemistry [17-20], biochemistry [21-24], and other material chemistry [25-28]. The development of physics to elucidate their structures and properties also contributes greatly [29-31]. In these development, chemistry, which supports the diversity of substances produced, and physics, which elucidates their structures and properties, offer one

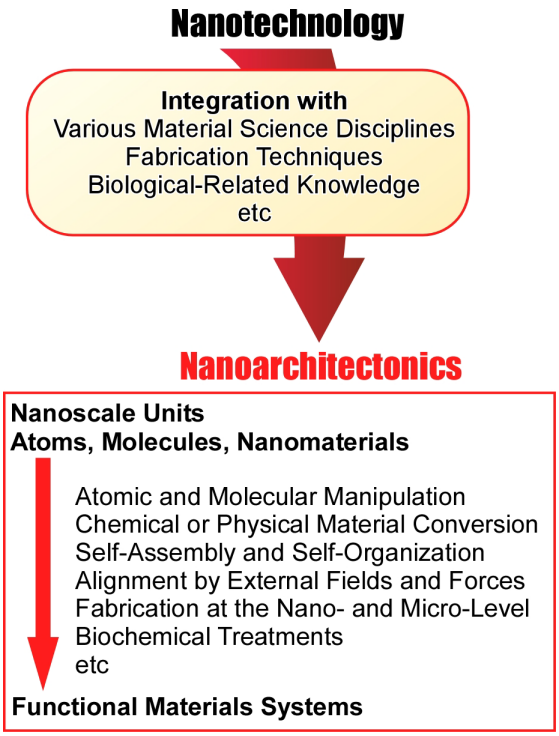

Figure 1. Outline of nnoarchitectonics: development from nanotechnology (top) and ways for preparation od functional materials systyems (bottom).

conclusion. It is not only the substances themselves, but also their microstructure that greatly influences its properties. The key to the development of functional materials is not only the production of materials but also the control of their nanostructure [32-34].

The decisive factor in this trend was the development of nanotechnology. Nanotechnology is still advanced concept in current materials science. It enables observation and manipulation at the atomic and molecular level [35-37] and unravels the properties of such nanoscopic levels. Nanotechnology has elucidated scientific phenomena of various materials at the nano-level [38-40]. The next step in materials developments is to build up materials, especially condensed matter, based on such nanotechnology-based knowledge. Richard Feynman founded nanotechnology in the 20th century [41, 42], and then, at the beginning of the 21st century, Masakazu Aono proposed the concept of nanoarchitectonics [43, 44]. Therefore, nanoarchitectonics can be regarded as a post-nanotechnology concept [45, 46]. In nanoarchitectonics, functional material systems are architected from nanounits. *i.e.*, atoms, molecules, and nanomaterials (Figure 1) [47, 48]. In nanoarchitectonics approaches, various methods such as atomic and molecular manipulation, chemical or physical material conversion, self-assembly and self-organization, alignment by external fields and forces, fabrication at the nano- and micro-level, and bio-chemical treatments are successfully selected and combined to architect functional material systems [49, 50]. Since several processes are combined in nanoarchitectonics approaches, it is easy to create asymmetric and hierarchical structures [51]. This is a distinct feature that distinguishes it from self-assembly [52], which relies on a simple single equilibrium.

The concept of nanoarchitectonics is very general and does not specifically choose the material of interests. Essentially, all matter is made of atoms and molecules, and nanoarchitectonics is the concept to construct materials from atoms and molecules. Therefore, this methodology can be applied to production of all materials. In other words, it can be a method to create all substances. It may be likened to the theory of everything, the ultimate theory in physics [53]. Nanoarchitectonics could be the method for everything in materials science [54, 55]. In fact, if you look at papers advocating nanoarchitectonics, the scope of its coverage spread widely. It is used in basic research areas such as material synthesis [56-58], structure control [59-61], fundamental physics research [62-64], and rather basic biochemistry research [65-67]. On the other hand, the concept is also used in applied fields such as catalysis [68-70], sensors [71-73], devices [74-76], energy production [77-79], energy storage [80-82], environmental handling [83-85], drug delivery [86-88], cell and tissue engineering [89-91], and biomedical applications [92-94].

Rather than being a completely new concept, nanoarchitectonics is a concept that integrates established disciplines. It combines nanotechnology with various material science disciplines, fabrication techniques, and biological-related knowledge to create an integrated methodology [95]. Due to its inclusive nature, previously known methods can also be considered part of nanoarchitectonics. For example, the creation of supramolecular assemblies [96-98], template synthesis to produce porous materials [99-101], the creation of ordered structures such as metal-organic frameworks (MOFs) [102-104] and covalent organic frameworks (COFs) [105-107], self-assembled monolayers (SAM) [108-110], Langmuir-Blodgett (LB) films [111-113], layer-by-layer (LbL) assembly [114-116], etc., can also be included in the nanoarchitectonics method.

Nanoarchitectonics is a very broadly addressed and integrated concept. It is difficult to describe it all in a single review paper. Here, this review would like to focus on layered structures in terms of structure formation. The unit structures of layered structures are mostly 2D materials or thin-film materials. They have attracted much attention in modern condensed matter science [117-119]. By organizing them into layered structures, we can expect to develop functions based on communication between the layers. Moreover, building up layered functional structures by assembling nano-layers of units is a typical approach in nanoarchitectonics. So far, we have discussed the characteristics of nanoarchitectonics based

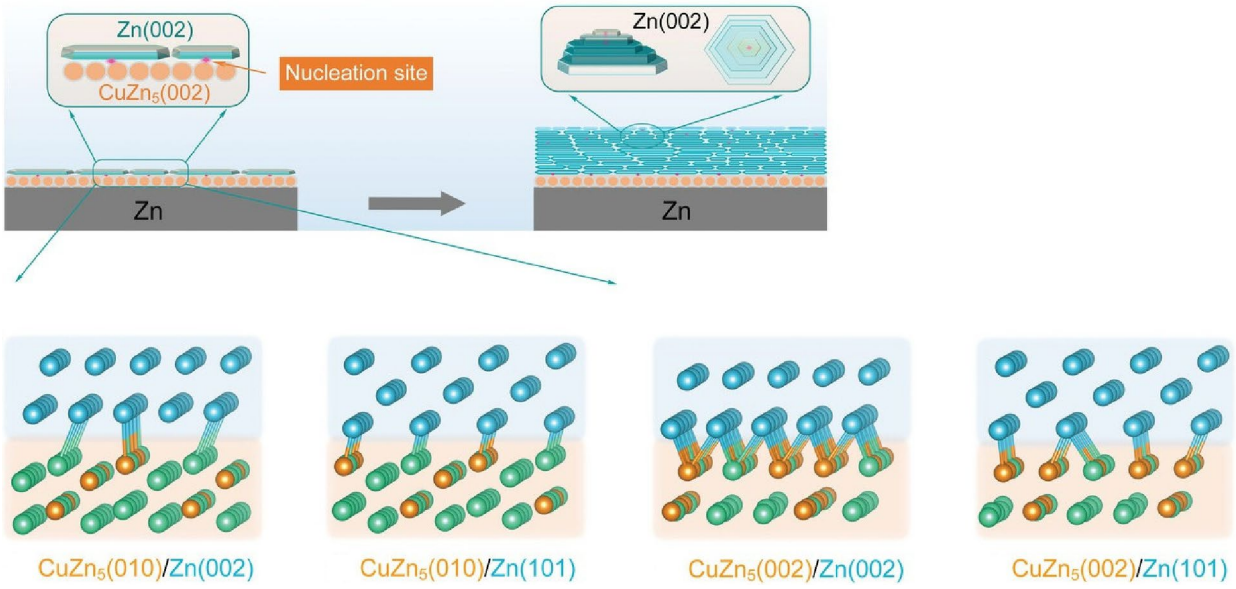

Figure 2. Schematic illustration of $CuZn_5$ alloy as an interfacial lattice lock layer to regulate the orientation of Zn deposits top) with calculation models of Zn(002) and Zn(101) nucleated on the surface of $CuZn_5$ planes. Reprinted with permission from Ref. 126 Copyright 2023 Wiley-VCH.

on methods such as the LB [120-122] and LbL methods [123-125]. In contrast, this review will discuss it according to the classification based on the characteristics of the constituent elements. Specifically, the discussion will be divided into the following categories: hard matter, hybrid, soft matter, and living object. For each target, several recent research examples will be given to illustrate the discussion. This paper will extract what aspects are considered important in the creation of the layered structure of each component. It will also discuss the properties of the functionality brought about in this context. Finally, what is needed to further develop the nanoarchitectonics of layered structures is discussed.

2. Hard matter

Among the stacked structures of various materials, this section will discuss some examples of hard matter layer stacking. The examples discussed are not necessarily representative or exhaustive. However, some features can be extracted. In layer structures of hard matter, the structural system at the atomic level has a significant impact on the functionality. Therefore, nanoarchitectonics that can control such structural systems is required. Physical thin film preparation methods are taken rather than methods such as chemisorption. Control of the interface of multilayered structures is of interest.

Layered nanoarchitectonics with hard matters is often useful on energy-relater applications. For example, the fabrication of a stable Zn/electrolyte interface is essential for the development of Zn-metal rechargeable batteries with long-term stability. This requires dense Zn electrodeposited nanoarchitectonics. To this end, Qie and co-workers constructed an interfacial lattice lock layer by electrodepositing Zn and Cu on a Zn electrode [126]. It is a Zn-containing interfacial lattice lock layer firmly attached to the Zn electrode surface and designed for planar Zn electrodeposition. The interfacial lattice-locked layer has the advantage of suppressing the lattice mismatch between the Zn(002) plane, selectively locking the lattice orientation of the Zn deposit and allowing layer-by-layer epitaxial growth of the Zn deposit. In their report, the Zn deposition behavior on this interfacial lattice-locked layer electrode is better analyzed. With the interface lattice lock layer, the growth of Zn nuclei is guided by stacking epitaxial growth due to the small lattice mismatch between Zn and $CuZn_5$. As a result, highly oriented horizontal hexagonal structure of Zn plating is possible. In the first stage of Zn plating, the exposed (002) face of $CuZn_5$ acts as a hetero nucleation source leading to Zn(002) nucleation and epitaxy. Figure 2 shows the control mechanism of the $CuZn_5$ alloy as an interfacial lattice lock layer on the Zn(002) crystal orientation. In the next step, the initially formed (002) textured Zn is used as a homogeneous nucleation source. Accordingly, further epitaxial growth of Zn(002) planes is induced, and finally a uniform and dense Zn plating layer is formed on the interfacial lattice lock layer electrode. The orientation-inducing and strong adhesion properties observed here enable stable Zn plating/peeling without dendrites in symmetric Zn||Zn cells. Despite the limited Zn supply,

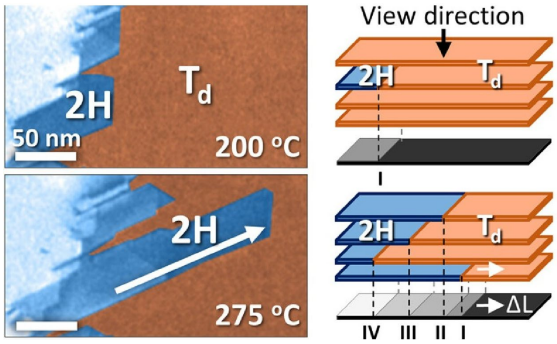

Figure 3. Micro- to atomic-scale phase transition by in situ heating in a TEM chamber: schematic of the intensity differences of 4-layer $MoTe_2$ 2H−Td interfaces where the mono-, bi-, tri-, and quadlayer 2H phase fronts are labeled as I, II, III, and IV, respectively. Reprinted with permission from Ref. 127 Copyright 2023 American Chemical Society.

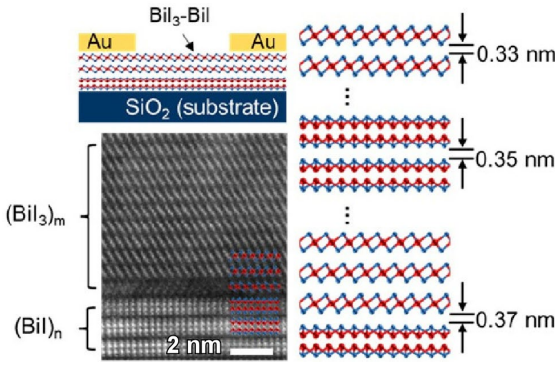

Figure 4. Layered van der Waals crystals constructed by alternating layers of two different layered structures: schematic diagram of the device structurewith cross-section TEM image of the BiI_3−BiI heterostructure and atomic structure diagram of BiI_3−BiI along [100] direction. Reprinted with permission from Ref. 130 Copyright 2023 American Chemical Society.

capacity retention after long-term cycling was observed$_2$. This methodology will provide new insights into the interface design of Zn electrodes. I paves the way for the practical application of Zn-metal batteries.

It is necessary to analyze in detail the two-dimensional (2D) materials that are the building blocks of layered functional structures. This will require the development of advanced observation and analysis methods as well as nanoarchitectonics. In particular, understanding the mechanisms of phase transitions in 2D materials is key to precisely tuning their properties at the nanoscale. For example, molybdenum ditelluride ($MoTe_2$) is a useful material for observing phase change behavior because it exhibits multiple phases at room temperature. Lee, Huang, and co-workers fabricated a lateral 2H-T_d interface by laser irradiation [127]. They then investigated the micro- to atomic-scale phase transition by in situ heating in a TEM chamber (Figure 3). To study the reversible phase transition of $MoTe_2$ from the microscale to the atomic scale, a combination of in situ TEM and graphene encapsulation was used. Using laser irradiation and thermal annealing, they have confirmed that a reversible phase transition between the semiconducting 2H and T_d phases can be achieved in a few layers of encapsulated $MoTe_2$. First, laser irradiation is used to locally convert a few-layer $MoTe_2$ flake from the 2H phase to a mixed phase of 1T′ and Td phases. Next, in-situ pulsed heating was applied, and the reversed phase transition from the T_d phase to the 2H phase was observed using a combination of scanning transmission electron microscope (STEM) and dark-field transmission electron microscopy (DFTEM). As a result, the T_d to 2H phase transition was found to initiate at the 2H-T_d interface around 200-225 °C. A highly anisotropic phase transition was observed between 200-400 °C. The 2H phase front progressed layer-by-layer along the b axis of the T_d crystal grains. Visualization of each 2H phase front enabled measurement of the T_d-2H phase transition kinetics of individual $MoTe_2$ layers. The phase transition between the 2H and T_d phases was also shown to be reversible by repeated laser irradiation and vacuum heating. The methodology presented here can be applied to micro- to atomic-scale in situ studies of solid-state phase transitions. The precisely fabricated layered nanoarchitecture is expected to have a variety of applications. For example, in coplanar 2D circuits including 2D Josephson junctions, broadband photodetectors, and other heterophase devices.

The contribution of 2D van der Waals materials and their heterostructures is immeasurable [128, 129]. They have great potential for optoelectronic and photonic applications. However, photodetectors and optoelectronic devices to date have relied on relatively simple van der Waals heterostructures with one or two blocks. Higher-order heterostructures are difficult to realize due to the difficult re-stacking and sequential synthesis of conventional layer-by-layer techniques. Mu et al. have developed an approach to directly exfoliate high-quality BiI_3-BiI heterostructured nanosheets with alternating blocks from solution-grown binary heterocrystals [130]. As shown in Figure 4, layered van der Waals crystals are constructed by alternating layers of two different layered structures. BiI_3-BiI nanosheets with this layered structure have typical type II energy band alignment properties. Crystals when grown show a regular hexagonal shape and are large in size. Crystallinity is high. BiI_3-BiI thin films were produced by a simple mechanical exfoliation process. This heterostructure also has potential for flexible and imaging applications. For example, it can be used as a channel

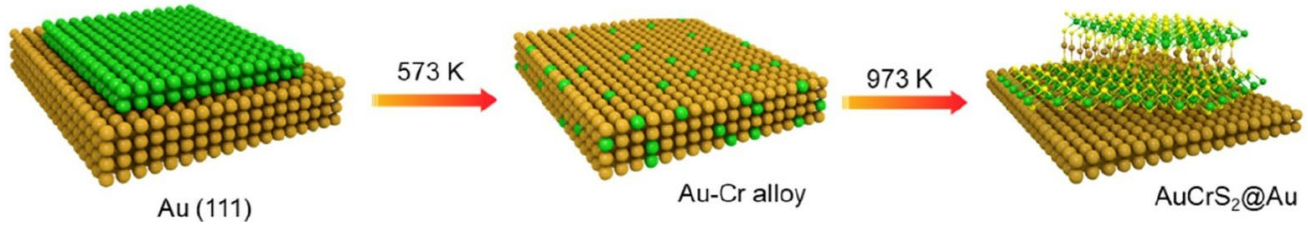

Figure 5. Schematic of the mechanism of growth of $AuCrS_2$ on Au where the orange, green, blue, and yellow spheres represent Au, Cr, Mo, and S atoms, respectively. Reprinted with permission from Ref. 132 Copyright 2024 American Chemical Society

material for photodetectors in a metal-semiconductor-metal configuration. This photodetector achieves extremely low dark currents, extraordinary detection rates, and fast response times. This approach expands the possibilities of van der Waals heterostructures. It will facilitate the development of high-performance optoelectronic devices. Alternating van der Waals heterostructures could be applied to low power consumption, fast response, and flexible optoelectronics. It could also provide insight into the fundamental physics of 2D van der Waals heterostructures.

In remote epitaxy, the polarity of the substrate penetrates the 2D materials and acts on the epilayer. However, the role of 2D materials in remote epitaxy is less clear. Xu, Cao, and co-workers studied the realization of remote epitaxy of single-crystal thin films on the weakest polarity/ionic substrate [131]. As a 2D material, graphene facilitates decaying charge transfer from the substrate to the epilayer. In addition, it brings about remote interaction. Interfacial atoms are assembled into incommensurate epitaxial relationships through graphene. It reduces misfit dislocations in the epilayer. Graphene reduces atomic transfer barriers, leading to a trend toward layer-by-layer growth modes. Accordingly, graphene has been demonstrated to play an important role in remote epitaxy. In particular, it is beneficial for fast growth of epilayers and reduction of dislocations at coalescence boundaries. This research will make remote epitaxy a major contribution to epitaxial growth technology. It lays the foundation for device applications of 2D material and semiconductor integration. It provides more valuable guidance for the effective use of 2D materials for nanoarchitectonics of 3D materials for device applications.

2D Non-layered transition metal dichalcogenide materials provide a platform for a variety of potential applications ranging from catalysis to quantum devices. Their synthetic nanoarchitectonics have not always been fully explored. Liu and co-workers reported the synthesis of 2D non-layered $AuCrS_2$ by gold-assisted chemical vapor deposition (Figure 5) [132]. The $AuCrS_2$ units grow in layers on top of the first CrS_2 monolayer. There, Au is bonded to the adjacent CrS_2 monolayer. Atomic-scale characterization of $AuCrS_2$ reveals that it consists of an Au layer sandwiched between two layers of CrS_2. This follows a layer-by-layer growth mechanism of CrS_2-$AuCrS_2$-$AuCrS_2$. This structure formation mechanism is supported by ab initio molecular dynamics simulations of the thermodynamics and kinetics of growth in the early stages, where Cr plays a key role in increasing the mobility of Au species and enhancing the adsorption energy of Au on CrS_2. This mechanism thus aids growth throughout the chemical vapor deposition process. The end result is a 2D non-layered material nanoporous $AuCrS_2$. The resulting freestanding nanoporous $AuCrS_2$ exhibits outstanding electrocatalytic properties for the hydrogen evolution reaction. The examples presented here encourage further studies of the exotic physical and chemical properties of 2D materials obtained by this unique nanoarchitectonics process.

3. Hybrid

Hybrids are also attractive materials because they combine the precise structure and functionality of inorganic materials with the flexibility of organic and/or bio materials [133-135]. Research on nanoarchitectonics of hybrid materials into layered structures is exemplified below.

Nanoarchitectonics of hybrid materials work efficiently on delicate controls of physical properties. Wu, Xie, Zhang, and co-workers achieved by nanoarchitectonics of layered structures on the metal nanocluster surface (Figure 6) [136]. They reported that by rigidifying the metal nanocluster surface and propagating the strain to the metal core, the vibration of the metal kernel is efficiently suppressed and the luminescence intensity is enhanced. Specifically, layer-by-layer triple ligand surface engineering enabled the nanoarchitectonics of solution-phase gold nanoclusters with strong fluorescence dominated by the metal core, up to high absolute quantum yields. This structure has a significant effect on the low-frequency acoustic vibration of the metal kernel. As a result, the vibration amplitude is reduced, although the vibration frequency is subtly changed. This inhibits the nonradiative relaxation of electron dynamics and causes the gold nanoclusters to exhibit strong luminescence. This nanoarchitectonics approach exemplifies the link between the

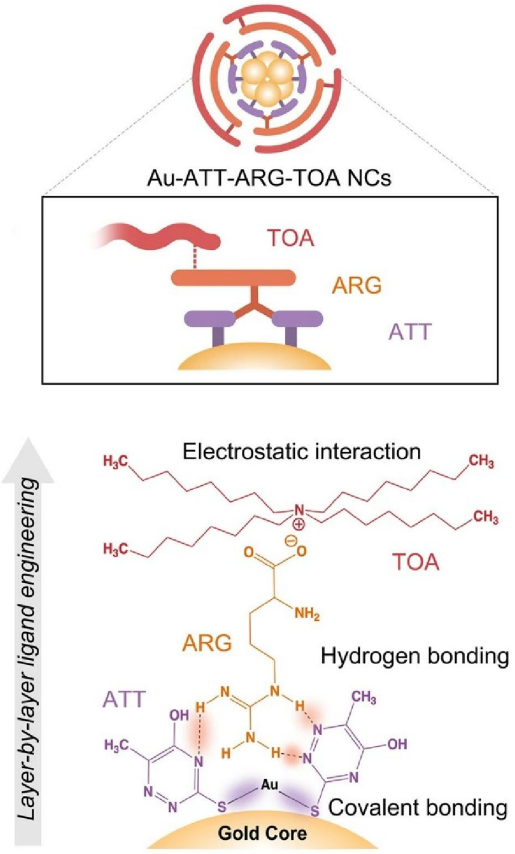

Figure 6. Supression of the vibration of the metal kernel through rigidifying the metal nanocluster surface and propagating the strain to the metal core with layer-by-layer triple ligand surface engineering for enhancement of luminescence intensity. Reproduced under terms of the CC-BY license from Ref. 136, 2023 Springer-Nature.

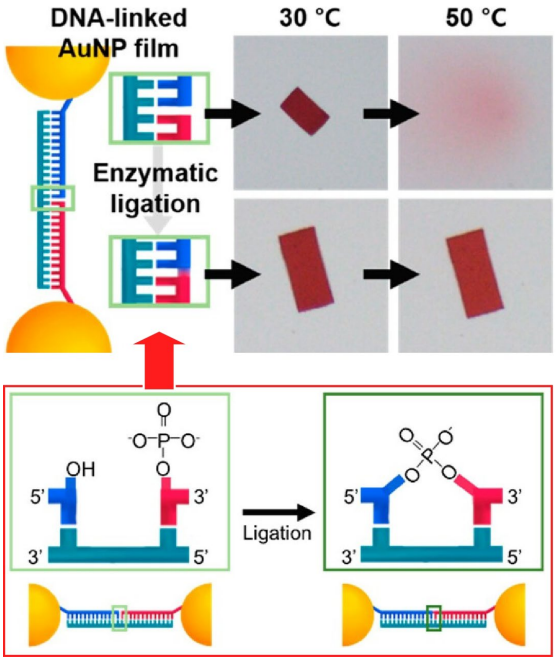

Figure 7. Site-directed enzyme ligation and DNA-based layer-by-layer thin film fabrication to fabricate DNA-bound gold nanoparticle films for stable shape morphing. Reprinted with permission from Ref. 140 Copyright 2024 American Chemical Society.

surface chemistry of metal nanoclusters and inner-shell state luminescence. They propose a strategy to make metal nanoclusters emit brightly by controlling the inner-shell motion inside the metal nanoclusters. The layer-by-layer triple-ligand self-assembly strategy is expected to expand its practical applications as it is exemplified in metal nanoclusters in diverse colloidal environments.

As a biomolecule, DNA is attractive as a soft component to form functional hybrids [137-139]. In addition, DNA sequencing is highly programmable. DNA also allows for highly responsive molecular recognition properties. Park and co-workers have used site-directed enzyme ligation and DNA-based layer-by-layer thin film fabrication [140]. They employed site-specific enzymatic ligation of DNA to fabricate DNA-bound gold nanoparticle films that exhibit stable shape morphing under conditions that normally cause unwinding of the DNA duplex (Figure 7). The enzymatic ligation method allows selective cross-linking. The used structure can be designed for flexibility in layer-by-layer assembly of DNA-based gold nanoparticles, selective enzymatic ligation of DNA, and photothermal etching to create the structure. Then, a free standing gold nanoparticle film with stably bound DNA strands was prepared. This thin film remained intact even under extreme conditions such as pure water and high temperatures that cause dissociation of the DNA duplex strand. In response to various environmental changes and DNA exchange reactions, the films exhibited reversible shape changes. For example, a change in solvent composition caused a color change from red to blue in single domain membranes. In addition, isotropic size contraction and expansion were induced. Multidomain coordination membranes responded to changes in ionic strength and DNA strand exchange reactions. The resulting membranes exhibited reliable rolling and unrolling behavior. Furthermore, selective enzymatic ligation could be combined with photothermal patterning to fabricate complex nanostructures. DNA-derived nano-actuators based on these structures could lead to the development of life-like robotic systems with increasingly complex structures and functions.

As in the previous example, soft actuators are of great interest for the next generation of soft robots. The need for effective sensing and expanded multitasking capabilities based on real-time feedback and self-regulation capabilities

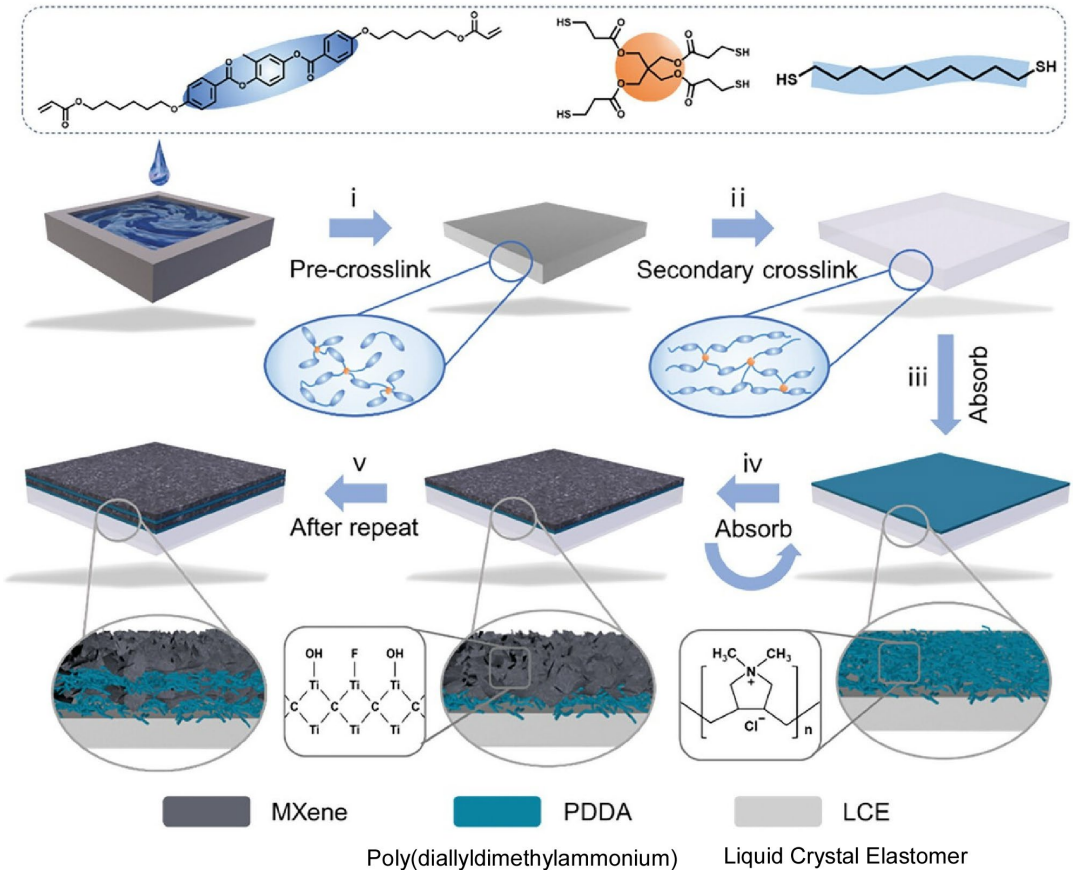

Figure 8. Fabrication of MXene/PDDAlayer-by-layer structures on a liquid crystal elastomer film. Reproduced under terms of the CC-BY license from Ref. 141, 2024 Wiley-VCH.

has prompted Niu, Liu, and co-workers to develop MXene/PDDA (poly(diallyldimethylammonium) layer-by-layer structures on a liquid crystal elastomer film (Figure 8) [141]. This fabricated a near-infrared-driven bimorph membrane with self-sensing and feedback-loop control functions. In this layered nanoarchitectonics approach, the actuator and sensing materials are attached to the bilayer film. The result is a highly accurate, self-sensing, feedback-loop control function. This is because potential delamination due to elastic modulus mismatch at the interface between the sensing and actuator layers is prevented. When the actuator is irradiated with near infrared light, which is also considered a closed-loop control system in the actuator, the alternating laminate membrane contracts and operates, changing its resistance accordingly. A microcontroller unit receives the signal of the resistance change, identifies it, and issues a command to modulate the near infrared laser irradiation. Due to its photothermal effect and high electrical conductivity, the laminated structure can sense its own motion state as well as react to light. Control of the near-infrared laser enables grasping, traction, and crawling actuator movements. For example, a light-driven dragonfly was assembled. When stimulated by a near infrared laser, the dragonfly is heated and its wings are driven by the self-sensing and closed-loop control functions. This research provides a new strategy for developing soft actuators that integrate self-sensing and actuation functions. It demonstrates the potential in the field of bionic robotics, artificial muscles, and intelligent soft actuators.

As porous hybrid materials, metal-organic frameworks (MOFs) have attracted much attention [142-144]. In particular, the preparation of MOF thin films firmly anchored on suitable substrates is useful for electronic and optical devices. A number of studies have been carried out, including the investigation of MOF thin films obtained by layer-by-layer assembly. Wöll, Knebel, and co-workers reported a fast method for preparing surface MOF (MIL-68(In)) layers on Au surfaces under harsh conditions (Figure 9) [145]. Using a dynamic layer-by-layer synthesis method, thin films with thicknesses tunable between 50 and 2000 nm could be nanoarchitectonically prepared in only 60 min. The first step was to create a self-assembled monolayer of 11-mercapto-1-undecanol on a quartz crystal microbalance (QCM) substrate used as a substrate. The MOF thin films were induced on the

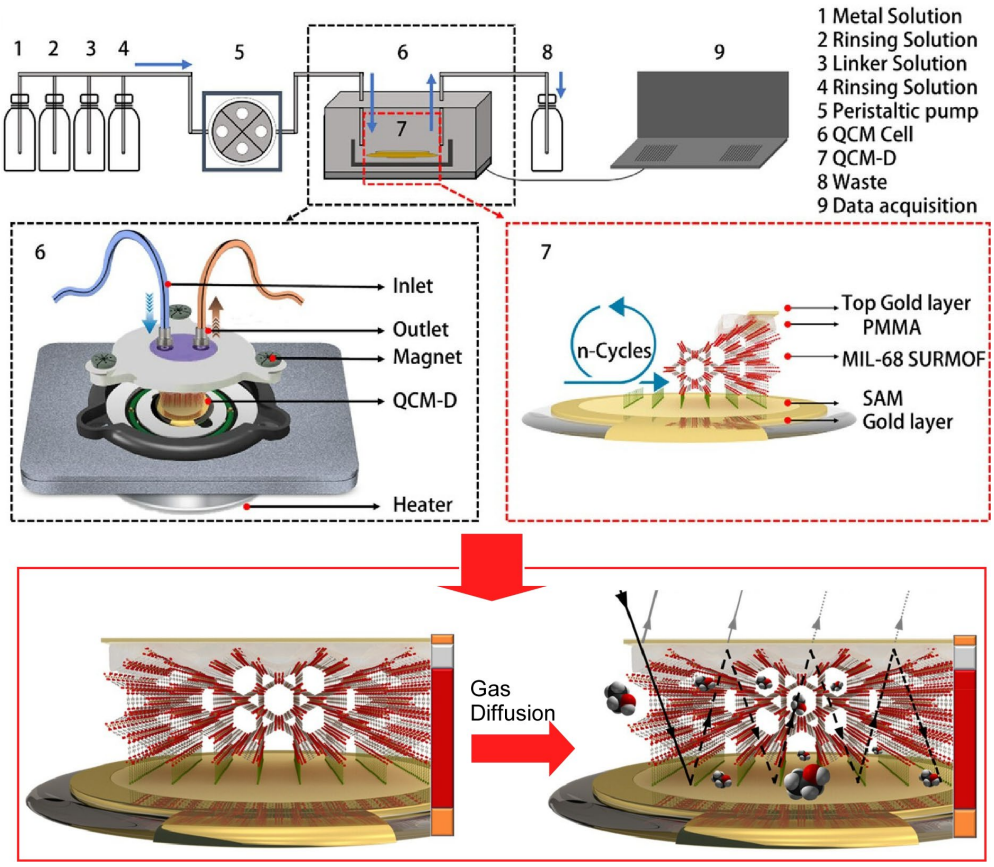

Figure 9. Afast method for preparing surface MOF (MIL-68(In)) layers on Au surfaces of QCM substrate by a continuous pumping cycle using alternating metal precursor solution (top) and Fabry-Pérot-type interferometers with a noticeable shift in the resonance point due to the change in the refractive index of the MOF caused by exposure to volatile compounds. Reprinted with permission from Ref. 145 Copyright 2023 American Chemical Society.

QCM substrate by a continuous pumping cycle using alternating metal precursor solution (indium nitrate in *N*,*N*-dimethylformamide (DMF)), organic linker solution (1,4-benzenedicarboxylic acid in DMF) and DMF. The continuous-flow LbL technique was used. This continuous flow LbL technique has the advantage of highly controllable thickness and short layering times. This is a useful approach for scalable thin film coatings. Structural analysis revealed that the pore channels of the MOFs are oriented parallel to the support. It was also found that these thin films exhibit extremely high optical quality. To create Fabry-Pérot-type interferometers, Au mirrors (about 10 nm) were sputtered after spin-coating with a polymethyl methacrylate layer (about 450 nm). A noticeable shift in the resonance point was observed due to the change in the refractive index of the MOF caused by exposure to volatile compounds. All cavity modes shifted to the higher wavelength side when exposed to the gas. Toluene shifted and broadened the resonance. In ethanol, the shifted resonances remained sharp. In general, this shift was more than sufficient to identify the analyte. The characteristic resonance signal change allows selective detection of chemical gases and vapors, where a series of resonances up to 10th order can be detected. As a result, host-guest interactions could be sensed through optical constant differences in the device. These multilayers with MOF cavities are suitable as light-reading sensors.

Chiral MOFs in circularly polarized optics have also been investigated. Wöll, Gu, and co-workers prepared monolithic, highly oriented chiral MOF thin films by a layer-by-layer method (Figure 10) [146]. In addition, they fabricated a circularly polarized light detection device to identify the enantiomers. A pair of enantiomeric linkers, R- and S-Cu(BDA) (BDA = 2,2-dihydroxy-1,1-binaphthalene-5,5-dicarboxylic acid), was used as chiral structures. [100] crystalline orientation was used to accumulate two-dimensional chiral MOF thin films. Samples were ethanol washed to remove any remaining unreacted reactants. A total of 30 cycles were used to grow the films, which were grown on SiO_2/Si substrates. The MOF thin films have a chiral, highly oriented monolithic structure with high optical quality.

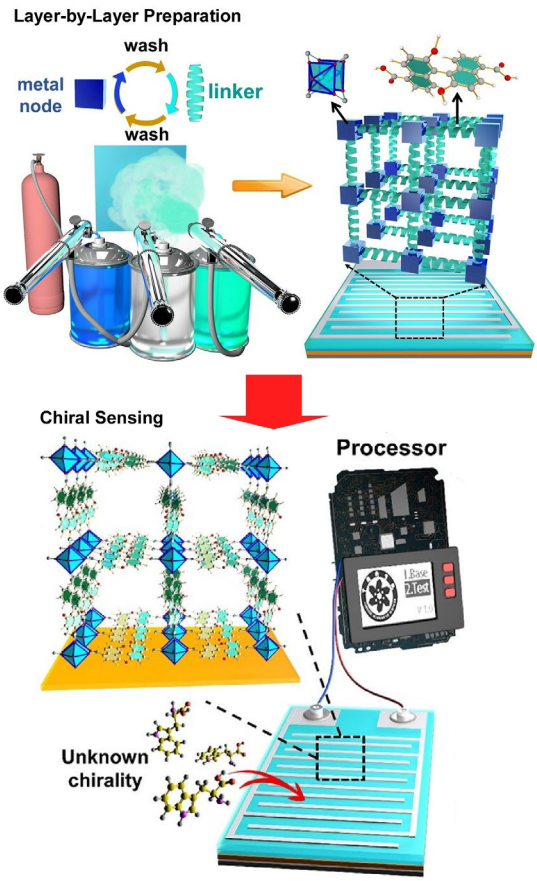

Figure 10. Preparation of monolithic, highly oriented chiral MOF thin films by a layer-by-layer method (top) and detection device to identify the enantiomers (bottom). Reprinted with permission from Ref. 146 Copyright 2023 American Chemical Society.

It shows outstanding sensitivity to the helicity of incident light. The chiral MOF thin film shows marked differences in the uptake of l- and d-tryptophan enantiomers. The films were molded into chirality-aware portable sensor devices that can monitor photocurrent signals. This work opens a new field of application for highly efficient circularly polarized light detection of enantiomers.

2D-Conjugated MOFs have excellent charge transport properties, which are derived from their unique layering structure with extended in-plane conjugation, and are promising materials for optoelectronic applications. The further development of MOF-based optoelectronics requires the development of high-quality, novel 2D-conjugated MOF thin films. Song et al. reported that Cu-HHHATN (HHHATN: hexahydroxyl-hexaazatrinaphthylene) was as a 2D-conjugated MOF [147]. It is characterized by high in-plane conjugation, strong interlayer π-π stacking, and multiple coordination sites. Large-area Cu-HHATN thin films with preferential orientation, high uniformity, and smooth surfaces were prepared using a simple layer-by-layer growth method (Figure 11). First, a hydroxyl group is introduced to the substrate. Next, the substrate is immersed in an ethanol solution of $Cu(OAc)_2$ to fix Cu^{2+} ions to the hydroxyl groups. The substrate is then immersed in an ethanol solution of HHATN ligand to form a continuous 2D-conjugated MOF film. A top-gate field-effect transistor (FET) based on the 2D-conjugated MOF thin film was fabricated as a flexible photodetector. Carrier mobility measurements showed typical bipolar behavior due to conduction processes through the tail state. A broadband optical response from ultraviolet to near infrared was demonstrated. The broadening of the optical response to 1450 nm at photon energies below the optical band gap was attributed to the hopping of photocarriers between gap states. Relatively long relaxation times are observed as a result of photocarrier trapping by defects. This relatively long relaxation time of the photocurrent results in synaptic plasticity of this device. This is analogous to biological synapses and has potential applications in neuromorphic visual systems. It provides a promising opportunity for the development of advanced flexible optoelectronic devices with multiple functions.

MOF materials have attracted much attention as a platform for solid-state chemistry or as a heterogeneous catalyst. Improving the light transparency and light-harvesting efficiency of MOFs by reducing light scattering and internal filtering effects due to microcrystallization could pave the way for photochemical and photocatalytic applications. Bloch, Powers, and co-workers have reported thin films of optically transparent, photochemically active, porous salts with layer-by-layer growth was reported (Figure 12) [148]. In this approach, optically transparent thin films consisting of porous molecular cages and photochemically active small molecules are assembled. MOF layered films are grown by sequential adsorption of cationic Zr-based porous coordination cages and anionic Mn porphyrins via LbL assembly. Molecules in the porous matrix can be efficiently site-isolated, where in situ optical spectroscopy allows real-time observation of chemical processes at the confined metal sites. Specifically, photoreduction, ligand exchange, and O_2 activation processes are all observed in real time. Photolysis promotes efficient reduction of Mn(III) sites to Mn(II) sites, while substrate access to the Mn(II) sites is enabled by the porous nature, facilitating reversible O_2 activation in the solid state. These results make optically transparent porous thin films a versatile platform for solid-state photochemistry and operando spectroscopy. It is expected that this materials platform will serve to expand the potential of solid-state photochemistry and facilitate further progress in heterogeneous catalysis research.

4. Soft matter

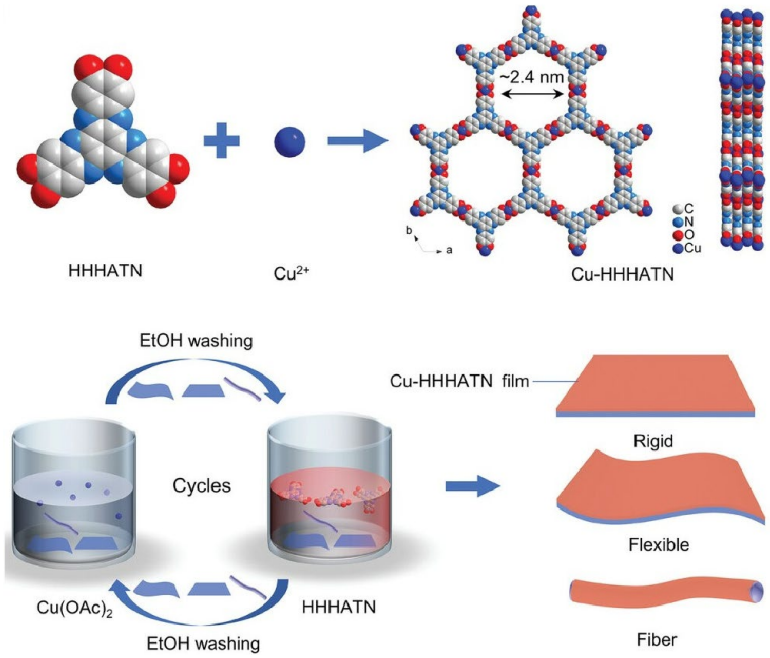

Figure 11. Large-area 2D-conjugated MOF thin film with preferential orientation, high uniformity, and smooth surfaces prepared using a simple layer-by-layer growth method. Reproduced under terms of the CC-BY license from Ref. 147, 2024 Wiley-VCH.

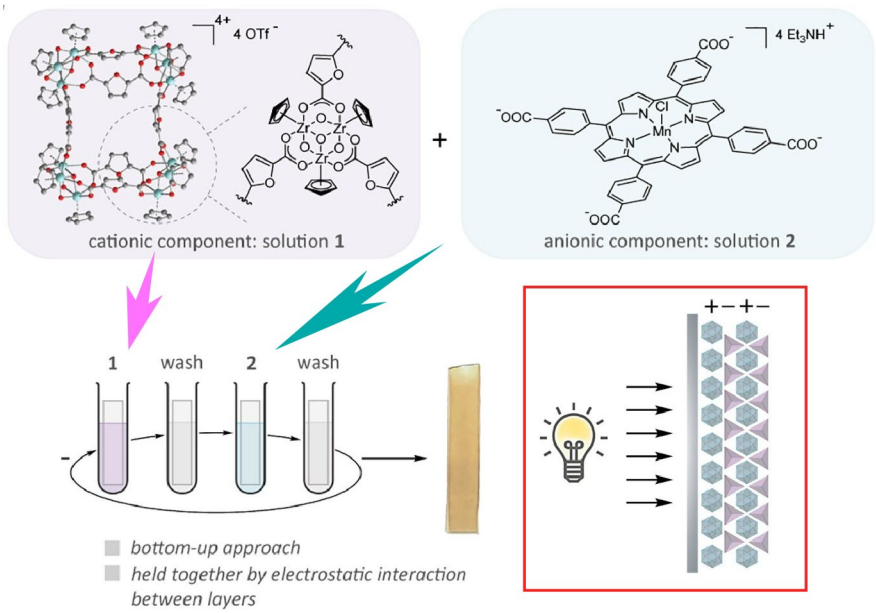

Figure 12. Preparation of thin films of optically transparent, photochemically active, porous salts with layer-by-layer growth by sequential adsorption of cationic Zr-based porous coordination cages and anionic Mn porphyrins via LbL assembly. Reproduced under terms of the CC-BY license from Ref. 148, 2023 American Chemical Society.

Although the differentiation from hybrid materials is not entirely clear, layered materials with high organic content, such as polymers, exhibit soft behavior as soft matter. They often exhibit flexible performance, including material flow,

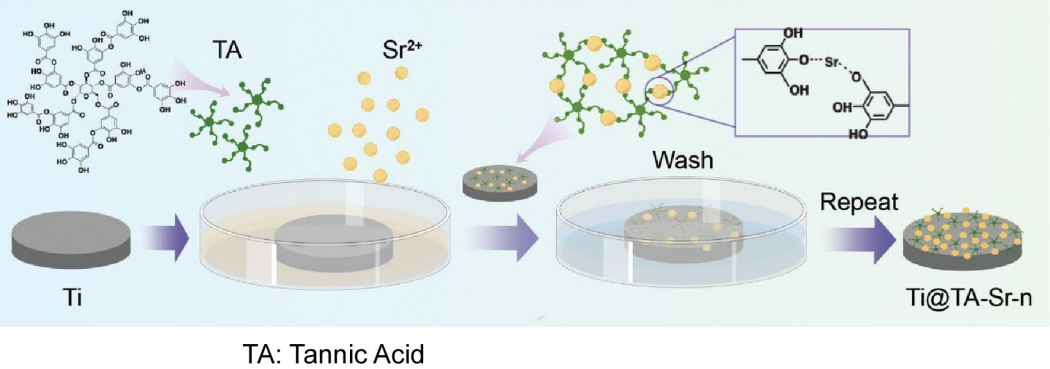

Figure 13. Preparation of metal-phenolic networks as multifunctional nanocoatings on titanium implants for improvement of osseointegration through early immunomodulation. Reproduced under terms of the CC-BY license from Ref. 149, 2024 Wiley-VCH.

movement, and change. Some examples analogous to such layered structures are summarized below.

Nanoarchitectonics of soft matters are often useful for functional coating as seen in osseointegration, which induces the direct bond between titanium and bone. Surface modification is an important factor to improve osseointegration of intraosseous implants. Therefore, the development of simple and efficient coating strategies is desirable. Han, Li, Ge, and co-workers reported metal-phenolic networks as multifunctional nanocoatings on titanium implants (Figure 13) [149]. This nanocoating aims to improve osseointegration through early immunomodulation. The metal-phenol network coating was nanoarchitectonized in layer by layer fashion on the titanium substrate surface by repeated incubation of the titanium substrate in tannic acid and Sr^{2+} solution. Tannic acid has catechol and galloyl groups. Thus, they can be easily chelated with a variety of metal ions. It also has a polyhydroxy structure that acts as a hydrogen bonding acceptor and donor. This structure allows it to interact with a variety of bioactive substances and to adhere to both hydrophilic and hydrophobic surfaces. Metal-phenol network coating composed of tannic acid and Sr^{2+} promotes initial adhesion and mobilization of bone marrow mesenchymal stem cells. It provides a bioactive interface that deflects macrophages to the M2 phenotype. In addition, the tannic acid-Sr coating promoted osteogenic differentiation of bone marrow mesenchymal stem cells. In vivo evaluation showed that it promoted osseointegration of implants by creating a favorable bone immune microenvironment. The metal-phenolic network structure also functions to load a variety of therapeutic agents. Therapeutic agents are delivered through the implant placement process to address a variety of needs. This will also help prevent and treat common clinical implant-related complications such as peri-implantitis. Tannic acid-Sr coating is a promising method of implant surface modification to achieve better and faster osseointegration. It may also be readily available for clinical applications.

A polymer electrolyte capacitor is a small solid-state capacitor that uses the transfer of unipolar ions in a single polymer electrolyte layer sandwiched between metal electrodes. Barillaro and co-workers layered anionic and cationic polyelectrolytes film between metal electrodes to create an amphipolar nanopolymer meter-thick (down to 10 nm) multilayers to create dielectrics (Figure 14) [150]. Using this structure, they report a multilayer polymer electrolyte capacitor that eliminates resistive behavior at frequencies from kHz to MHz. The first step is to functionalize a gold-coated glass slide with self-assembled monolayers of 11-mercaptoundecanoic acid to immobilize a negative charge on the surface. Nanometer-thick polyelectrolyte LbL films, i.e., multilayer layered films of positively charged poly(vinyltrimethylammonium chloride) and negatively charged poly(sodium styrenesulfonate), are nanoarchitected on gold-coated slides using electrostatic interaction. Polyelectrolyte multilayers were examined with different number of layers: 10, 20, and 40 layers. The bipolar multilayer polymer electrolyte capacitors exhibited full capacitive behavior from 100 mHz to 10 MHz. Satisfying the requirements for the use of polymer electrolyte capacitors in most industrial and consumer electronics applications, they operated reliably over time for more than 300 million cycles, at different bias voltages up to 3 V, and at temperatures up to 80°C, and exhibited reversible capacitive behavior without significant hysteresis. It is expected that this bi-polar nanometer-thick polyelectrolyte dielectric will be used to fabricate flexible electronic devices that operate at high frequencies, such as capacitors and field-effect transistors.

Polymerization of layered structures with a defined structure allows nanoarchitectonics of 2D conjugated microporous polymers. Goto and co-workers solved this problem by free radical solid phase polymerization of

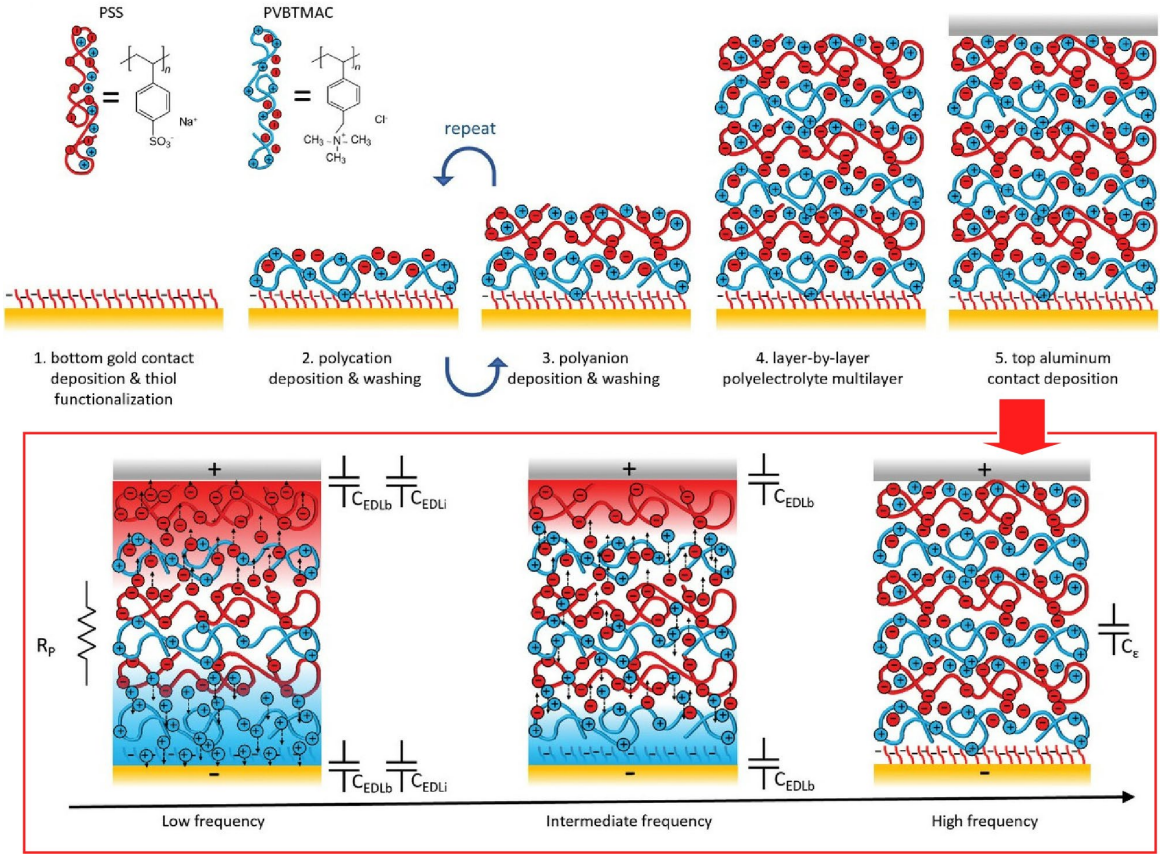

Figure 14. Ptreparation of layered anionic and cationic polyelectrolytes film between metal electrodes to create an amphipolar nanopolymer meter-thick multilayers to create dielectrics (top) for multilayer polymer electrolyte capacitor that eliminates resistive behavior at frequencies from kHz to MHz (bottom). Reprinted with permission from Ref. 150 Copyright 2024 Wiley-VCH.

acetylenes (Figure 15) [151]. In this approach, acetylene monomers are co-crystallized using halogen bonding. The polymerization was based on the structure of the obtained co-crystals. Importantly, the acetylene monomers are aligned in the co-crystal so that adjacent C≡C groups are far enough apart to effectively undergo radical polymerization. Even when acetylene monomers with low radical reactivity are used, high molecular weight polyacetylene, which cannot be obtained by solution phase radical polymerization, can be obtained. After polymerization, removal of the linker moiety produced a 2D conjugated microporous polymer with structurally designed pores. The pore size can be tuned by changing the linker. This 2D conjugated microporous polymer showed very high adsorption capacity for Li^+ and B^{3+}, and can be expected to be an environmentally friendly adsorbent.

In order to extend the battery life of aqueous zinc-ion batteries, side reactions in the metallic zinc anode need to be considered in depth. Fan, Song, and co-workers presented a methodology to create an ion-conductive, mechanically robust electrolyte/anode interface and stabilize zinc anodes using LbL self-assembly technology (Figure 16) [152]. The LbL film used in this research is composed of biodegradable biopolymers, chitosan and sodium alginate. With this LbL film, no obvious dendrites were observed after long-term cycling in both symmetric and perfect cells. The polymer used in this research is rich in hydroxyl groups. It adsorbs strongly to the metal anode surface to form a protective layer. As a result, the metal anodes can be separated from the bulk electrolyte. The LbL layer composed of chitosan and sodium alginate is thought to interact via hydrogen bonds between the functional groups of the polyelectrolyte and the zinc ions. Density functional theory calculations suggest that the desolvation energy of the zinc ions on the anode surface is reduced. The LbL method is inherently cost-effective, and taking into account the environmental suitability of the materials used, this Zn protection strategy could lead to industrial applications for aqueous zinc-ion batteries.

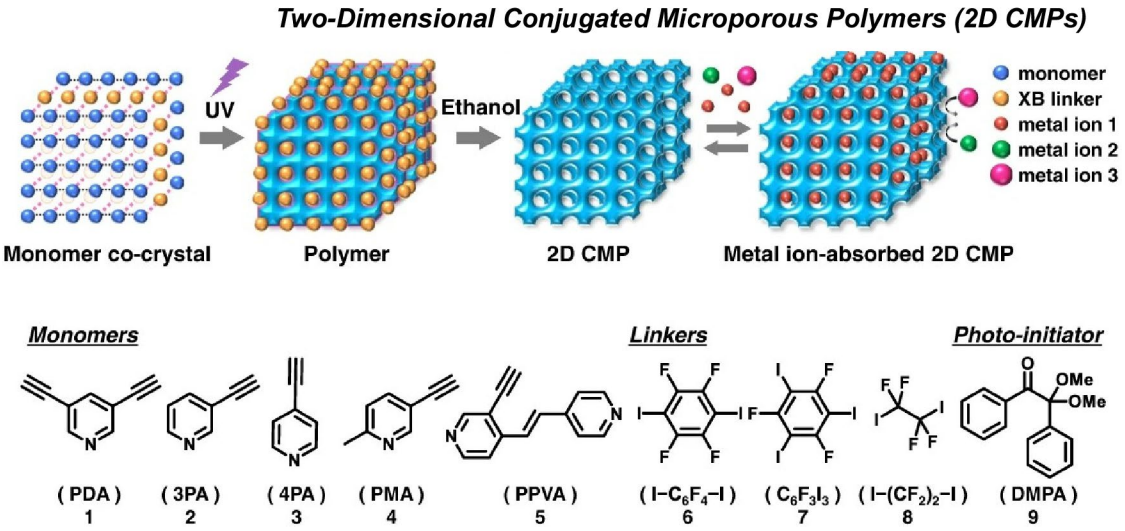

Figure 15. Free radical solid phase polymerization of acetylenes in co-crystal via halogen bonding where the acetylene monomers are aligned in the co-crystal so that adjacent C≡C groups are far enough apart to effectively undergo radical polymerization followed by removal of the linker moiety to produce a 2D conjugated microporous polymer with structurally designed pores. Reproduced under terms of the CC-BY license from Ref. 151, 2023 Springer-Nature.

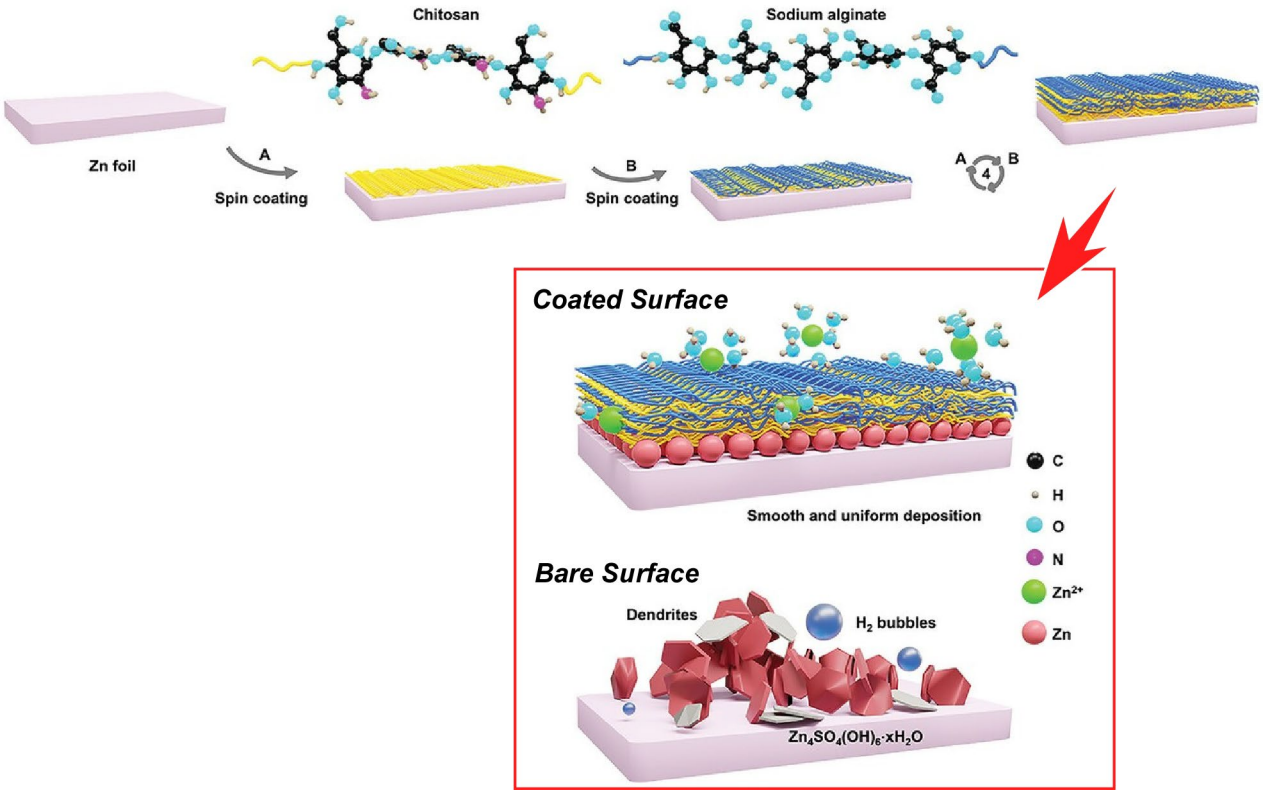

Figure 16. Stabilization of zinc anodes using LbL self-assembly technology composed of chitosan and sodium alginate. Reprinted with permission from Ref. 152 Copyright 2024 Wiley-VCH.

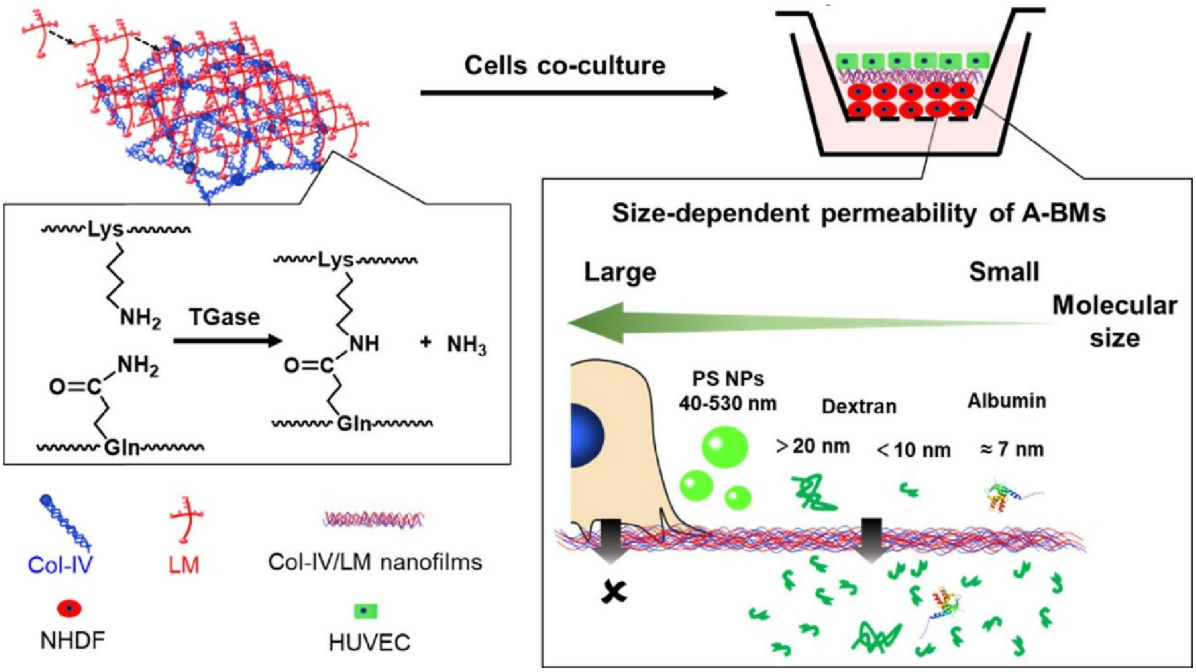

Figure 17. Crosslinked LbL nanofilms of type-IV collagen (Col-IV) / laminin (LM) in situ in 3D tissues where the material permeability is in good agreement with the known size-selective behavior of glomerular basement membranes: NHDF, normal human dermal fibroblasts; HUVEC, human dmbilical vein endothelial cell. Reprinted with permission from Ref. 156 Copyright 2020 American Chemical Society.

Technology to integrate electronic circuits in layers is also necessary for development informational functional materials. Photolithography is a promising technique to realize multilayered electronic circuits. However, when using thick stretchable nanocomposite conductors, photolithography is difficult to employ because of the opaque nature of this material. Ko, Jeon Lee, and co-workers have devised a photothermal lithography technique that can pattern elastomeric conductors and via holes using a pulsed laser [153]. Stretchable nanocomposite conductors patterned by photothermal lithography is created based on a percolation network formed by spatial heating of the laser. The conductors and via holes are repeatedly patterned. This allows for layer-by-layer nanoarchitectonics of highly conductive and durable multilayer circuits. A stretchable wireless pressure sensor and a passive matrix light emitting diode array are also nested. The potential of stretchable multilayer electronic circuit configurations with multi-functionality, durability, and high density was demonstrated.

5. Living object

The concept of a functional layered structure can be extended to one in which the material is a living cell. Some examples of such ultimate layered structure creation and their functions are shown below. Depending on the method, living cells can also be molded into multilayered structures like materials.

LbL assembly is useful for this purpose. Matsusaki and coworkers report several examples of multilayering of living cells by the LbL method and related techniques [154, 155]. Living systems, highly organized tissues, rely on the compartmentalizing effect of basement membranes that separate different types of cells. For example, Matsusaki and coworkers crosslinked LbL nanofilms of type-IV collagen/laminin in situ in 3D tissues with transglutaminase [156]. This created a strong artificial basement membrane (Figure 17). This is in situ cross-linking of nanofilms in living 3D tissue. This artificial basement membrane is stable. It also has a stronger barrier effect to maintain the cellular compartment of the organized 3D tissue. The material permeability was in good agreement with the known size-selective behavior of glomerular basement membranes. This in vitro artificial basement membranes aid in the fabrication of more complex compartmentalized 3D tissue designs. It also contributes to our understanding of cell-to-cell crosstalk through the basement membrane. It is also expected to provide reliable 3D tissue models for new drug screening and other in vitro physiological studies. For example, the use of type-IV collagen/laminin nanofilms as artificial basement membranes will help to understand specific diffusion processes in the kidney.

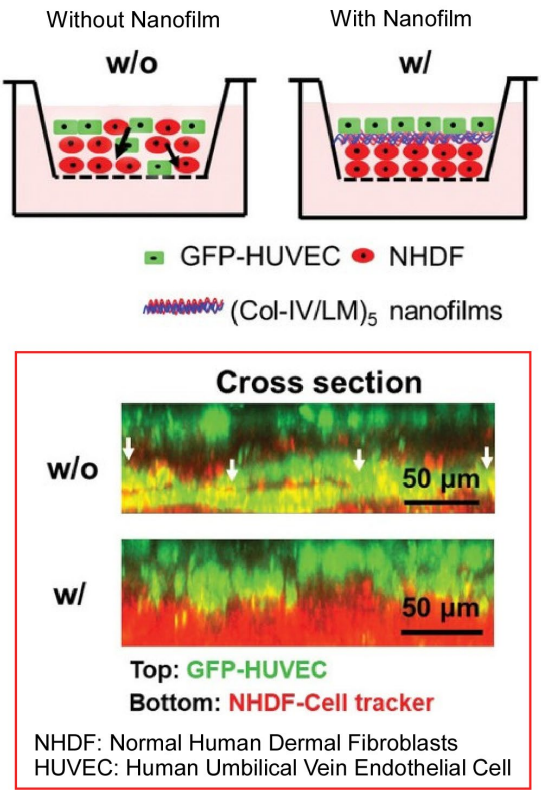

Figure 18. Multilayer type-IV collagen/laminin nanofilm for compartmentalized co-culture of fibroblasts and endothelial cells where the nanofilm works like a barrier with a separation effect, but with cross-talk between cells. Reprinted with permission from Ref. 157 Copyright 2020 Wiley-VCH.

Tissue engineering techniques are gaining attention in the creation of 3D tissues and organs. However, designed cell positions are easily lost as cells migrate during the cell culture period. In the human body, the basement membrane maintains precise 3D cellular positions. This can be described as compartmentalized. It is very significant to construct an artificial basement membrane that mimics this good function. Matsusaki and co-workers have developed a type-IV collagen/laminin nanofilm layered structure as an artificial basement membrane [157]. The type-IV collagen/laminin nanofilms have high cell adhesion properties and effectively maintain their spreading morphology. The resulting multilayer nanofilms are tunable in composition, thickness, and fibrous network. The nanoarchitectonics can be made to resemble the properties of natural basement membranes. This multilayer type-IV collagen/laminin nanofilm allows compartmentalized co-culture of fibroblasts and endothelial cells. The nanofilm works like a barrier with a separation effect, but with cross-talk between cells (Figure 18). It has been shown that this nanofilm is capable of forming cellular compartments in 3D tissues. It could thereby become a more reliable tissue model for the evaluation of drug efficacy, nanotoxicology, and transplantation. In addition, the LbL assembly method is highly compatible with bioprinting. This will promote nanoarchitectonics of tissues with higher complexity of LbL nanofilms. Co-culture of user-defined artificial basement membranes and patterned cells could also be expanded to create compartmentalized 3D tissues that can meet a variety of demands.

The use of bottom-up tubular cell sheets without scaffolds has been proposed for promising therapies for patients with cardiovascular diseases. Chen, Lu, and co-workers reported a method for LbL assembly of naturally formed tubular cell sheets and further cell culture (Figure 19) [158]. This method also allowed them to successfully fabricate structured small-diameter artificial blood vessels consisting of three layers of tubular cell sheets with different cell types and arrangements. First, cylindrical substrates coated with surface-patterned collagen were fabricated. A near infrared photothermal conversion cylindrical mandrel was fabricated by adding polydimethylsiloxane/carbon nanotubes. The cylindrical mandrel was coated with a thermal phase-change collagen layer. In addition, its surface was patterned with a polydimethylsiloxane seal by photolithography. The patterned collagen layer facilitated cell adhesion and orientation. As a result, continuous tubular cell monolayers spontaneously formed after approximately 4 days of cell culture. Biocompatible near infrared light was used to induce a photothermal phase transition of the collagen coated on the cylindrical substrate to dissociate the collagen layer. As a result, intact tubular cell sheets could be harvested in a few minutes. The tubular cell sheets exhibited excellent self-supporting properties. This is an important trait from the viewpoint of operability and practical use. Fabrication of freestanding multilayered structured small caliber artificial vessels with different cell types and arrangements was also realized. The LbL assembly method of structured small-caliber artificial vessels is an extremely good technique for forming hierarchically structured artificial vessels. It is also easy to operate and has a short preparation time. This approach is promising for the repair of damaged vessels. This noninvasive strategy could be an innovation for tubular tissue fabrication in regenerative medicine.

One of the main possible advantages of cell sheet technology is that it allows for sustained cellular viability, survival, and repair function. It can thereby be used as a scaffold-free 3D cell delivery platform. The 3D tissue-like microenvironment inherent in cell sheets has been shown to stimulate paracrine factor production in mesenchymal stem cell. Kim, Okano, and co-workers reported a strategy of multilayering cell sheets by centrifugation [159]. This has the effect of noninvasively enhancing paracrine factor production by mesenchymal stem cells. First, they optimized the

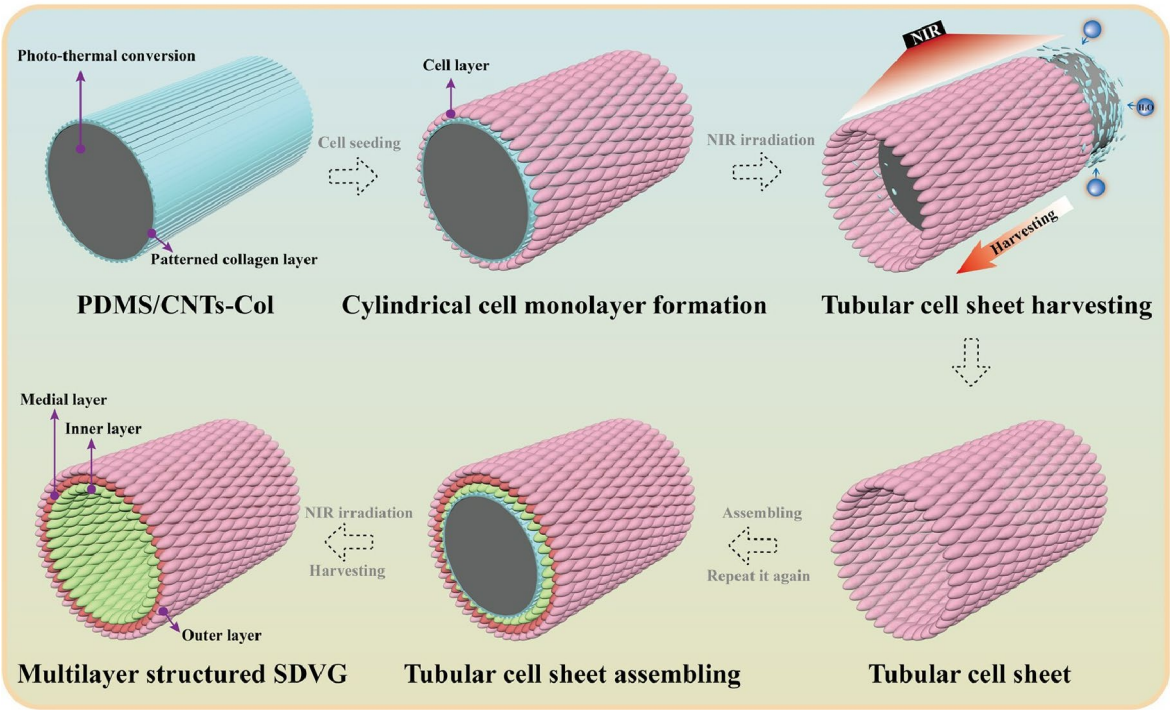

Figure 19. LbL assembly of naturally formed tubular cell sheets and further cell culture fabrication for structured small-diameter artificial blood vessels consisting of three layers of tubular cell sheets with different cell types and arrangements. Reprinted with permission from Ref. 158 Copyright 2023 American Chemical Society.

rotational speed and time to make the cell sheets produced by centrifugation into monolayers. Centrifugation has the effect of enhancing cellular physical and biochemical interactions related to intercellular communication and matrix interactions within a single cell sheet. Mesenchymal stem cell gene expressions of connexin 43, integrin β1, and laminin α5 were increased. Centrifugation of single cell sheets caused enhancement of mesenchymal stem cell function and secretion of high concentrations of the pro-regenerative cytokines vascular endothelial growth factor, hepatocyte growth factor, and interleukin-10. Cohesive bilayered mesenchymal stem cell sheets could be produced in only less than 2 hours by layering and centrifuging the cell sheets. Cell-cell interactions at the laminate-sheet interface can produce a variety of functions. For example, layering resulted in a 10-fold increase in vascular endothelial growth factor production. Cell-sheet centrifugal layering enhanced paracrine-related secretory function. This could be an easy method to fabricate scaffold-free 3D mesenchymal stem cell tissue-like constructs for regenerative medicine applications.

Smooth muscle cells are wall cells that perform important contractile functions in many tissues. Tissue abnormalities of smooth muscle cells are used in many diseases, including atherosclerosis, asthma, and uterine fibroids. However, the potential biological and physiological relevance of smooth muscle cell clusters has not yet been fully established. Wang, Barakat, and co-workers have combined in vitro experiments with physical modeling [160]. They found that 3D clusters of smooth muscle cells form when cell contractility punctures flat smooth muscle cell sheets. The subsequent evolution of clusters can also be modeled. The models consider the balance between the surface tension of the cluster resulting from both cellular contractility and adhesive forces and the viscous dissipation of the cluster. These factors can be modeled as an active dewetting process with shape evolution of clusters. Elucidating the physical mechanisms governing the spontaneous development of such 3D clusters may provide insight into smooth muscle cell-related diseases. It will be possible to study the influence of smooth muscle cell clusters on the development of atherosclerotic plaques and uterine fibroids. It could also allow the study of aspects of density-driven smooth muscle cell hypertrophy and hyperplasia. It could also serve as a useful in vitro model for these studies.

Owens, Kim, Jung, and co-workers have reported on the direct transfer of cell sheets from culture surfaces to target surfaces (Figure 20) [161]. This novel cell sheet nanoarchitectonics is by interfacial cell transfer between two surfaces with different cell adhesion properties. Commercially available flexible parylene was used as the culture surface. UV-treated parylene has various advantages. It has effective properties for both stable cell adhesion in culture and efficient cell migration to the target surface. Intermediate levels of cell

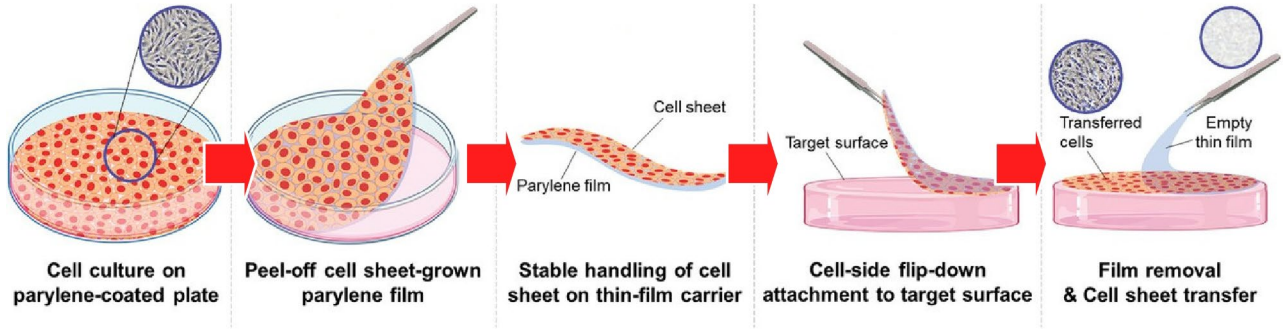

Figure 20. Direct transfer of cell sheets from culture surfaces to target surfacesupon interfacial cell transfer between two surfaces with different cell adhesion properties. Reprinted with permission from Ref. 161 Copyright 2022 Wiley-VCH.

adhesion are appropriate for these functions. First, cells were seeded onto UV-treated parylene-coated plates and cultured until a confluent monolayer was achieved. The 3-4 μm thick parylene film containing the cell sheets was peeled off the plate by cutting it with a surgical blade. The cell side of the film was then applied to the targeted area like a transfer tattoo sticker. The cell sheets could be transferred from the parylene film to a new surface with higher cell affinity. Interfacial cell migration occurs by utilizing transmembrane proteins present on the cell surface to bind to the target surface. Finally, the parylene film was peeled off without leaving any cells on the film side after the cell sheet adhered to the target surface. By repeating this process, they also succeeded in forming heteromorphic cell-sheet multilayers. Re-establishment and reversal of cell polarity after cell migration was also confirmed. The method was successfully applied to several cell types, including osteoblasts, myoblasts, endothelial cells, epithelial cells, and fibroblasts. In those cases, the polarity of the cells reversed during transplantation, too. Other features such as free-form design and curved surface application have also been demonstrated. The therapeutic potential of this cell sheet delivery system was investigated. Applications to skin wound healing and skin tissue regeneration in a mouse model were demonstrated. In the future, this cell delivery platform is expected to have therapeutic applications as a functional patient-specific cell patch.

6. Summary and perspectives

In this paper, we have collected examples of layered nanoarchitectonics of various materials. Layered structures are diverse, and it is not always easy to discuss them all in a comprehensive and systematic manner. Therefore, this paper has divided them into four categories: hard matter, hybrid, soft matter, and living object with listing some examples of recent research. While these examples do not cover all features, some features can be extracted. these features are briefly summarized below.

In the layered structure of hard matter, the structural system at the atomic level has a great impact on the functions. Nanoarchitectonics that can satisfy the high structural regime is required. Physics-based thin film preparation methods are often used rather than chemisorption and other techniques. In such cases, control of the layered structure, interface control, and characterization in the two-dimensional plane are of interest. The pursuit of the function of layered structures of hard matter also leads to the investigation of more fundamental physical phenomena in two-dimensional and layered systems. Layered structures of hybrid materials can also be created through complex formation between organic materials and metals. Hybrids are attractive materials for functional development because they combine the precise structure and functionality of inorganic materials with the flexibility of organic and biomaterials. Hybrid-type layered structure fabrication induces a diversity of functional components and structures, leading to various functional pioneering. Layered materials with high organic content, such as polymers, exhibit soft behavior as soft matter. Although the differentiation from hybrid materials is not entirely clear, they often exhibit flexible performance, including material flow, movement, and change. Soft matter layered structures can be fabricated in a variety of ways, but layer-by-layer assembly using component interactions is a particularly useful approach. Such versatile flexible layering can produce a variety of functions. The concept of layered structures of functionality can be extended to materials that are living cells. Depending on the method, living cells can also be molded into multilayered structures like materials. Living cells are themselves highly functional entities. They also have the property of moving on their own. In order to create functional layered structures with such living cells as functional units, it is important to use nanoarchitectonic means that allow the free exchange of signals, molecules, etc., while setting limits on their mobility.

As mentioned above, different components have different characteristics that make the nanoarchitectonics and

functional development of the layers different. The type of structural precision and functionality required is highly dependent on the flexibility and mobility of the component. Strategies need to be adapted to the characteristics of the components. Such a tactic is effective when building up a layered structure from somewhat similar components. However, the methodology needs to be further devised for layered nanoarchitectonics of different categories of components. To develop more advanced functional systems, it is necessary to assemble different categories of functional components in a layered fashion. Inevitably, the components become more complex in such challenges. Accordingly nanoarchitectonics may become more difficult. It may be difficult to be solved only with experimental experience and subject-specific theoretical approaches. In order to rationally combine many accumulated findings, an approach based on materials informatics is necessary [162, 163], such as selecting the optimal approach and predicting the properties of functional materials by machine learning [164-166]. In deed, there is also a proposal to integrate materials informatics with nanoarchitectonics [167, 168]. Nanoarchitectonics, which creates material structures from functional units, can be applied to various materials. On the other hand, materials informatics has the ability to handle a great deal of information. It is advantageous to use these versatile properties within the somewhat defined framework of layered structures to create functional material structures.

In a layered functional structure, the functions of the two-dimensional layers work together to allow signals, energy, and information to flow in an asymmetric, vectorial fashion. By organizing two-dimensional organization into layered structures, we can expect to develop functions based on communication between the layers. Combinations and sequences of such functional unit layer have to be logically designed from huge selective possibilities. Information-based technology would support this development. Accordingly, highly functional materials are expected to be created through the fusion of nanoarchitectonics and novel methodologies such as materials informatics.

Acknowledgements

This study was partially supported by Japan Society for the Promotion of Science KAKENHI (Grant Numbers JP20H00392 and JP23H05459).

References

[1] Segawa Y, Levine D R and Itami K 2019 *Acc Chem Res* **52** 2760
[2] Sugiyama M, Akiyama M, Yonezawa Y, Komaguchi K, Higashi M, Nozaki K and Okazoe T 2022 *Science* **377** 756
[3] Iwasawa N 2023 *Bull. Chem. Soc. Jpn.* **96** 824.
[4] Fujimoto H, Yasui K and Tobisu M 2023 *Bull. Chem. Soc. Jpn.* **96** 872
[5] Zhang E, Zhu Q, Huang J, Liu J, Tan G, Sun C, Li T, Liu S, Li Y, Wang H, Wan X, Wen Z, Fan F, Zhang J and Ariga K 2021 *Appl, Catal, B Environ.* **293** 120213,
[6] Islam M S, Yuta Shudo and Hayami S 2022 *Bull. Chem. Soc. Jpn.* **95** 1
[7] Yadav N, Gaikwad R P, Mishra V and Manoj B. Gawande M B 2022 *Bull. Chem. Soc. Jpn.* **95** 1638
[8] Soontornchaiyakul W, Yoshino S, Kanazawa T, Haruki R, Fan D, Nozawa S, Yamaguchi Y and Kudo K 2023 *J. Am. Chem. Soc.* **145** 20485
[9] Larasati L, Lestari W W and Firdaus M 2022 *Bull. Chem. Soc. Jpn.* **95** 1561
[10] Su Y, Otake K, Zheng J-J, Horike S, Kitagawa S and Gu C 2022 *Nature* **611**, 289
[11] Ay B, Takano R and Ishida T 2023 *Bull. Chem. Soc. Jpn.* **96**, 1129–1138
[12] Takezawa H, Iizuka K and Fujita M 2024 *Angew. Chem. Int. Ed.* **63**, e202319140
[13] Liu C, Morimoto N, Jiang L, Kawahara S, Noritomi T, Yokoyama H, Mayumi K and Ito, K 2021 *Science* **372** 1078
[14] Watanabe S and Oyaizu K 2023 *Bull. Chem. Soc. Jpn.* **96** 1108
[15] Yang W, Mixich L, Boonstra, F and Cabral H 2023 *Adv. Healthcare Mater.* **212**, 2202688.
[16] Furukawa Y and Shimokawa D 2023 *Bull. Chem. Soc. Jpn.* **96** 1243
[17] Chen G, Sciortino F, Takeyasu K, Nakamura J, Hill J P, Shrestha L K and Ariga K 2022 *Chem. Asian J.* **17** e202200756.
[18] Matsuno T and Isobe H 2023 *Bull. Chem. Soc. Jpn.* **96**, 406
[19] Kubota R 2023 *Bull. Chem. Soc. Jpn.* **96** 802
[20] Morishita D, Yoshimitsu Itoh Y, Furukawa K, Arai N, Xu-Jie Zhang X-J and Aida T 2024 *Chem. Sci.* **15**, 4068
[21] Jia Y, Yan X and Li J 2023 *Angew. Chem. Int. Ed.* **61** e202207752
[22] Murayama K, Okita H and Asanuma H 2023 *Bull. Chem. Soc. Jpn.* **96** 1179
[23] Hayashi T 2023 *Bull. Chem. Soc. Jpn.* **96** 1331
[24] Kalyana Sundaram S d, Hossain M M, Rezki M, Ariga K and Tsujimura S 2023,*Biosensors* **13** 1018
[25] Adschiri T, Takami S, Umetsu M, Ohara S, Naka T, Minami K, Hojo D, Togashi T, Arita T, Taguchi M, Itoh M, Aoki N, Seong G, Tomai T and Yoko A 2023 *Bull. Chem. Soc. Jpn.* **96**, 133
[26] Shinde P A, Abbas Q, Chodankar N R, Ariga K, Abdelkareem M A and Olabi A G 2023 *J. Energy Chem.* **79**, 611
[27] Fukuoka A 2023 *Bull. Chem. Soc. Jpn.* **96**, 1071
[28] Ishii M, Yamashita Y, Watanabe S, Ariga K and Takeya J 2023 *Nature* **622** 285
[29] Kimura K, Miwa K, Imada H, Imai-Imada M, Kawahara S, Takeya J, Kawai M, Galperin M and Kim Y 2019 *Nature* **570** 210
[30] Terazima M 2023 *Bull. Chem. Soc. Jpn.* **96** 852
[31] Uematsu T, Krobkrong N, Asai K, Motomura G, Fujisaki Y, Torimoto T and Kuwabata S 2023 *Bull. Chem. Soc. Jpn.* **96** 1274
[32] Guo D, Shibuya R, Akiba C, Saji S, Kondo T and Nakamura J 2016 *Science* **351** 361

[33] Maeda K, Takeiri F, Kobayashi G, Matsuishi S, Ogino H, Ida S, Mori T, Uchimoto Y, Tanabe S, Hasegawa T, Imanaka N and Kageyama H 2022 *Bull. Chem. Soc. Jpn.* **95** 26

[34] Imahori H 2023 *Bull. Chem. Soc. Jpn.* **96** 339

[35] Sugimoto Y, Pou P, Abe M, Jelinek P, Pérez R, Morita S and Custance O 2007 *Nature* **446** 64

[36] Negi S, Mami Hamori M, Kitagishi H and Kano K 2022 *Bull. Chem. Soc. Jpn.* **95** 1537

[37] Harano K, Nakamuro T and Nakamura E 2024 *Microscopy* **73** 101

[38] Tokoro H, Nakabayashi K, Nagashima S, Song Q, Yoshikiyo M and Ohkoshi S 2022 *Bull. Chem. Soc. Jpn.* **95** 538

[39] Kobayashi Y, Yokota Y, Takahashi Y, Takeya J and Yousoo Kim Y 2023 *J. Phys. Chem. C* **127** 13929

[40] Hashikawa Y and Murata Y 2023 *Bull. Chem. Soc. Jpn.* **96** 943

[41] Feynman R P 1960 *California Inst. Technol. J. Eng. Sci.* **4**, 23

[42] Roukes M 2001 *Sci. Am.* **285** 48

[43] Ariga K, Ji Q, Nakanishi W, Hill J P and Aono M 2015 *Mater. Horiz.* **2** 406

[44] Ariga K and Aono M 2016 *Jpn. J. Appl. Phys.* **55** 1102A6.

[45] Ariga K 2021 *Nanoscale Horiz.* **6** 364

[46] Ariga K 2022 *Small Methods* **6** 2101577

[47] Ariga K 2022 *Nanoscale* **14** 10610

[48] Song J, Kawakami K and Ariga K 2023 *Curr. Opin. Colloid Interface Sci.* **65** 101702

[49] Ariga K, Li J, Fei J, Ji Q and Hill J P 2016 *Adv. Mater.* **28** 1251

[50] Ariga K, Mori T, Kitao T and Uemura T 2020 *Adv. Mater.* **32** 1905657.

[51] Ariga K, Jia X, Song J, Hill J P, Leong D T, Jia Y and Li J 2020 *Angew. Chem. Int. Ed.* **59** 15424.

[52] Ariga K, Nishikawa M, Mori T, Takeya J, Shrestha L K and Hill J P 2019 *Sci. Technol. Adv.Mater.* **20** 51

[53] Laughlin R B and Pines D 2020 *Proc. Natl. Acad. Sci.* **97** 28

[54] Ariga K and Fakhrullin R 2022 *Bull. Chem. Soc. Jpn.* **95** 774

[55] Ariga K 2024 *Bull. Chem. Soc. Jpn.* **97** uoad001

[56] Dalui A, Ariga K and Acharya S 2023 *Chem. Commun.* **59** 10835

[57] Han M, Kani K, Na J, Kim J, Bando Y, Ahamad T, Alshehri S M and Yamauchi Y 2023 *Adv. Funct. Mater.* **33** 2301831.

[58] Shinde P A and Ariga K 2023 *Langmuir* **39** 18175

[59] Chen G, Shrestha L K and Ariga K 2021 *Molecules* **26** 4636

[60] Hikichi R, Tokura Y, Igarashi Y and Imai H 2023 *Bull. Chem. Soc. Jpn.* **96** 766

[61] Eftekhari K, Parakhonskiy B V, Grigoriev D and Skirtach A G. 2024 *Materials* **17** 1051

[62] Nayak A, Unayama S, Tai S, Tsuruoka T, Waser R, Aono M, Valov I and Hasegawa T 2018 *Adv. Mater.* **30** 1703261

[63] Eguchi M, Nugraha A S, Rowan A E, Shapter J and Yamauchi Y 2021 *Adv. Sci.* **8** 2100539

[64] Cao L, Huang Y, Parakhonskiy B and Skirtach A G 2022 *Nanoscale* **14** 15964

[65] Ariga K, Ji Q, Mori T, Naito M, Yamauchi Y, Abe H and Jonathan P. Hill J P 2013 *Chem. Soc. Rev.* **42** 6322

[66] Komiyama M, Yoshimoto K, Sisido M and Ariga K 2017 *Bull. Chem. Soc. Jpn.* **90**, 967

[67] Shen X, Song J, Sevencan C, Leong D T and Ariga K 2022 *Sci. Technol. Adv. Mater.* **23** 199

[68] Chen G, Sciortino F and Ariga K 2021 *Adv. Mater. Interfaces* **8** 2001395.

[69] Chen G, Singh S K. Takeyasu K, Hill J P, Nakamura J and Ariga K 2022 *Sci. Technol. Adv. Mater.* **23** 413

[70] Sharma D, Choudhary P, Mittal P, Kumar S, Gouda A and Krishnan V 2024 *ACS Catal.* **14** 4211

[71] Ishihara S, Labuta J, Van Rossom W, Ishikawa, D, Minami K, Hill J P and Ariga K 2014 *Phys. Chem. Chem. Phys.* **16,** 9713

[72] Komiyama M, Mori T and Ariga K 2018 *Bull. Chem. Soc. Jpn.* **91** 1075

[73] Chen G, Bhadra B N, Sutrisno L, Shrestha L K and Ariga K 2022 *Int. J. Mol. Sci.* **23** 5454

[74] Zhou F, Zhao Y, Fu F, Liu L and Luo Z 2023 *Crystals* **13** 1506

[75] Tsuchiya T, Nakayama T and Ariga K 2022 *Appl. Phys. Express* **15** 100101

[76] Azzaroni O, Piccinini E, Fenoy G, Marmisollé W and Ariga K 2023 *Nanotechnology* **34** 472001

[77] Khan A H, Ghosh S, Pradhan B, Dalui A, Shrestha L K, Acharya S and Ariga K 2017 *Bull. Chem. Soc. Jpn.* **90** 627

[78] Sadanandan A M, Yang J-H, Devtade V, Singh G, Dharmarajan N P, Fawaz M, Lee J M, Tavakkoli E, Jeon C-H, Kumar P and Vinu A 2024 *Prog. Mater. Sci.* **142** 101242

[79] Kim D, Lim H, Kim S H, Lee K N, You J, Ryu D Y and Kim J 2024 *J. Mater. Chem. A* **12** 7452

[80] Kim J, Kim J H and Ariga K, 2017 *Joule* **1** 739

[81] Shinde P A, Nilesh R. Chodankar N R, Kim H-J, Abdelkareem M A, Ghaferi A A, Han Y-K, Olabi A G and Ariga K 2023 *ACS Energy Lett.* **8** 4474

[82] Druzian D M, Machado A K, Ourique A F and Da Silva W L 2024 *J. Mol. Liq.* **395** 123902

[83] Barreca D and Maccato C 2023 *CrystEngComm* **25**, 3968

[84] Huang P, Wu W, Li M, Li Z, Pan L, Ahamad T, Alshehri S M, Bando Y, Yamauchi Y and Xu X 2024 *Coord. Chem. Rev.* **501** 215534

[85] Agamendran N, Uddin M, Yesupatham M S, Shanmugam M, Augustin A, Kundu T, Kandasamy R, Sasaki K and Sekar K 2024 *Langmuir* **40**, 3320

[86] Nakanishi W, Minami K, Shrestha L K, Ji Q, Hill J P and Ariga K 2014 *Nano Today* **9** 378

[87] Ferhan A R, Park S, Park H, Tae H, Jackman J A and Cho N-J 2022 *Adv. Funct. Mater.* **32** 2203669.

[88] Komiyama M 2023 *Beilstein J. Nanotechnol.* **14** 218

[89] Hu W, Shi J, Lv W, Jia X and Ariga K 2022 *Sci. Technol. Adv. Mater.* **23** 393

[90] Tian B, Liu J, Guo S, Li A and Wan J-H 2023 *Int. J. Biol. Macromol.* **243** 125161

[91] Jia X, Chen J, Lv W, Li H and Ariga K 2023 *Cell Rep. Phys. Sci.* **4** 101251

[92] Duan H, Wang F, Xu W, Sheng G, Sun Z and Chu H 2023 *Dalton Trans.* **52** 16085

[93] Li B, Huang Y and Zou Q 2023 *ChemBioChem* **24** e202300002.

[94] Sutrisno L and Ariga K 2023 *NPG Asia Mater.* **15**, 21

[95] Ariga K 2023 *ChemNanoMat* **9** e202300120.

[96] Datta S, Kato Y, Higashiharaguchi S, Aratsu K, Isobe A, Saito T, Prabhu D D, Kitamoto Y, Hollamby M J, Smith A J, Dalgliesh R, Mahmoudi N, Pesce L, Perego C, Pavan G M and Yagai S 2020 *Nature* **583** 400

[97] Hamada K, Shimoyama D, Hirao T and Haino T 2022 *Bull. Chem. Soc. Jpn.* **95** 621

[98] Yamamoto Y, Kushida S, Okada D, Oki O, Yamagishi H and Hendra 2023 *Bull. Chem. Soc. Jpn.* **96** 702

[99] Malgras V, Ji Q, Kamachi Y, Mori T, Shieh, F-K, Wu K C-W, Ariga K and Yamauchi Y 2015 *Bull. Chem. Soc. Jpn.* **88** 1171

[100] Tiburcius S, Krishnan K, Patel V, Netherton J, Sathish C, Weidenhofer J, Yang J-H, Verrills N M, Karakoti A and Vinu A 2022 *Bull. Chem. Soc. Jpn.* **95** 331

[101] Pan Z-Z, Lv W, Yang Q-H and Nishihara H 2022 *Bull. Chem. Soc. Jpn.* **95** 611

[102] Troyano J, Horike S and Furukawa S 2022 *J. Am. Chem. Soc.* **144** 19475

[103] Ohata T, Tachimoto K, Takeno K J, Nomoto A, Watanabe T, Hirosawa I and Rie Makiura R 2023 *Bull. Chem. Soc. Jpn.* **96**, 274

[104] Horike S, 2023 *Bull. Chem. Soc. Jpn.* **96**, 887

[105] Matsumoto M, Valentino L, Stiehl G M, Balch H B, Corcos A R, Wang F, Ralph D C, Mariñas B J and Dichtel W R 2018 *Chem* **4** 308

[106] Charles-Blin Y, Kondo T, Wu Y, Bandow S and Awaga K 2022 *Bull. Chem. Soc. Jpn.* **95** 972

[107] Cao C, Chen Q, Suizu R and Awaga K 2024 *J. Mater. Chem. C* **12** 3072

[108] Kawasaki Y, Nakagawa M, Ito T, Imura Y, Wang K-H and Kawai T 2022 *Bull. Chem. Soc. Jpn.* **95**, 1006

[109] Sekimoto T, Yamamoto T, Takeno F, Nishikubo R, Hiraoka M, Uchida R, Nakamura T, Kawano K, Saeki A, Kaneko Y and Matsui T 2023 *ACS Appl. Mater. Interfaces* **15** 33581

[110] Cho S W, Pandey P, Yoon S, Ryu J, Lee D-G, Shen Q, Hayase S, Song H, Choi H, Ahn H, Oh C-M, Hwang I-W, Cho J S and Kang D-W 2023 *Surf. Interfaces B* **42**, 103478

[111] Ariga K, Yamauchi Y, Mori T and Hill J P 2013 *Adv. Mater.* **25** 6477

[112] Oliveira Jr. O N, Caseli L and Ariga K 2022 *Chem. Rev.* **122** 6459

[113] Negi S, Hamori M, Kubo Y, Kitagishi H and Kano K 2023 *Bull. Chem. Soc. Jpn.* **96** 48

[114] Lvov Y, Ariga K and Kunitake T 1994 *Chem. Lett.* **23** 2323

[115] Decher G 1997 *Science* **277** 1232

[116] Borges J, Zeng J, Liu X Q, Chang H, Monge C, Garot C, Ren K, Machillot P, Vrana N E, Lavalle P, Akagi T, Matsusaki M, Ji J, Akashi M, Mano J F, Gribova V and Picart C 2024 *Adv. Healthcare Mater.* **13** 2302713.

[117] Li C, Cao Q, Wang F, Xiao Y, Li Y, Delaunay J-J and Zhu H 2018 *Chem. Soc. Rev.* **47** 4981

[118] Liu A, Liang X, Ren X, Guan W, Gao M, Yang Y, Yang Q, Gao L, Li Y and Ma T, 2020 *Adv. Funct. Mater.* **30** 2003437.

[119] Fu J-H, Cai Y, Shen J, Sugisaki H, Nanjo K, To K, Wu C-W, Han Y, Li L-J and Tung V 2023 *Matter* **6** 2136

[120] Ariga K 2020 *Langmuir* **36** 7158

[121] Ariga K 2023 *Chem. Mater.* **35**, 14

[122] Ariga K 2023 *Small* 15636

[123] Rydzek G, Ji Q, Li M, Schaaf P, Hill, J P, Boulmedais F and Ariga K 2015 *Nano Today* **10** 138

[124] Ariga K, Lvov Y and Decher G 2022 *Phys. Chem. Chem. Phys.* **24** 4097

[125] Ariga K, Song J and Kawakami K 2024 *Chem. Commun.* **60**, 2152

[126] Ji J, Zhu Z, Du H, Qi X, Yao J, Wan H, Wang H, Qie L and Huang Y, 2023 *Adv. Mater.* **35** 2211961

[127] Lee C-H, Ryu H, Nolan G, Zhang Y, Lee Y, Oh S, Cheong H, Watanabe K, Taniguchi T, Kim K, Lee G-H and Huang P Y 2023 *Nano Lett.* **23** 677

[128] Joseph S, Mohan J, Lakshmy S, Thomas S, Chakraborty B, Thomas S and Kalarikkal N, 2023 *Mater. Chem. Phys.* **297** 127332,

[129] Pirabul K, Pan Z-Z, Tang R, Sunahiro S, Liu H, Kanamaru K, Yoshii T and Nishihara H 2023 *Bull. Chem. Soc. Jpn.* **96** 510

[130] Mu H, Zhuang R, Cui N, Cai S, Yu W, Yuan J, Zhang J, Liu H, Mei L, He X, Mei Z, Zhang G, Bao Q and Lin S 2023 *ACS Nano* **17** 21317

[131] Wang Y, Qu Y, Xu Y, Li D, Lu Z, Li J, Su X, Wang G, Shi L, Zeng X, Wang J, Cao B and Xu K 2023 *ACS Nano* **17** 4023

[132] Wang M, Chen D, Li Z, Wang Z, Huang S, Hai P, Tan Y, Zhuang X and Liu P 2024 *Nano Lett.* **24** 2308

[133] Ariga K, Akakabe S, Sekiguchi R, Thomas M L, Takeoka Y, Rikukawa M, and Yoshizawa-Fujita M 2024 *ACS Omega* **9** 22203

[134] Shichijo K, Watanabe M, Hisaeda Y and Shimakosh H 2022 *Bull. Chem. Soc. Jpn.* **95** 1016

[135] Li Z, Nakamura K and Kobayashi N 2023 *Bull. Chem. Soc. Jpn.* **96** 816

[136] Zhong Y, Zhang J, Li T, Xu W, Yao Q, Lu M, Bai X, Wu Z, Xie J and Zhang Y 2023 *Nat. Commun.* **14** 658

[137] Endo M. 2022 *Molecules* **27**, 4224.

[138] Juji S and Oishi M 2022 *Bull. Chem. Soc. Jpn.* **95** 410

[139] Roy B and Govindaraju T 2024 *Bull. Chem. Soc. Jpn.* **97** bcsj.20230224

[140] Choi J, Kim J, Park J-y, Hyun J K and Park S-J 2024 *Nano Lett.* **24** 2574

[141] Yang Y, Meng L, Zhang J, Gao Y, Hao Z, Liu Y, Niu M, Zhang X, Liu X and Liu S 2024 *Adv. Sci.* **11** 2307862.

[142] Shan Y, Zhang G, Yin W, Pang H and Xu Q 2022 *Bull. Chem. Soc. Jpn.* **95** 230

[143] Nishijima A, Kametani Y and Uemura T 2022 *Coord. Chem. Rev.* **466** 214601

[144] Moribe S, Takeda Y, Umehara M, Kikuta H, Ito J, Ma J, Yamada Y and Hirano M 2023 *Bull. Chem. Soc. Jpn.* **96** 321

[145] Monjezi B H, Okur S, Limbach R, Chandresh A, Sen K, Hashem T, Schwotzer M, Wondraczek L, Wöll C and Knebel A 2023 *ACS Nano* **17** 6121

[146] Tian Y-B, Tanaka K, Chang L-M, Wöll C, Gu Z-G and Jian Zhang J 2023 *Nano Lett.* **23** 5794

[147] Song J, Liu C-K, Piradi V, Chen C, Zhu Y, Zhu X, Li L, Wong W-Y and Yan F 2024 *Adv. Sci.* **11** 2305551

[148] Sur A, Simmons J D, Ezazi A A, Korman K J, Sarkar S, Iverson E T, Bloch E D and Powers D C 2023 *J. Am. Chem. Soc.* **145** 25068

[149] Liu J, Shi Y, Zhao Y, Liu Y, Yang X, Li K, Zhao W, Han J, Li J and Ge S 2024 *Adv. Sci.* **11** 2307269.

[150] Paghi A, Mariani S, Corsi M, Maurina E, Debrassi A, Dähne L, Capaccioli S and Barillaro G 2024 *Adv. Mater.* **36** 2309365
[151] Le H T, Wang C-G and Goto A 2023 *Nat. Commun.* **14** 171
[152] Cai X, Wang X, Bie Z, Jiao Z, Li Y, Yan W, Fan H J and Song W 2024 *Adv. Mater.* **36** 2306734.
[153] Song S, Hong H, Kim K Y, Kim K K, Kim J, Won D, Yun S, Choi J, Ryu Y-I, Lee K, Park J, Kang J, Bang J, Seo H, Kim Y-C, Lee D, Lee H, Lee J, Hwang S-W, Ko S H, Jeon H and Lee W 2023 *ACS Nano* **17** 21443
[154] Zenga J and Matsusaki M 2019 *Polym. Chem.* **10** 2960
[155] Shang Y, Zeng J, Xie Z, Sasaki N, and Matsusak M 2022 *Bull. Chem. Soc. Jpn.* **95** 1163
[156] Zeng J, Correia C R, Mano J F and Matsusaki M 2020 *Biomacromolecules* **21** 4923
[157] Zeng J, Sasaki N, Correia C R, Mano J F and Matsusaki M 2020 *Small* **16** 1907434
[158] Xu W, Yao M, He M, Chen S and Lu Q 2023 *ACS Appl. Mater. Interfaces* **15** 19966
[159] Bou-Ghannam S, Kim K, Kondo M, Grainger D W and Okano T 2022 *Cells* **11** 2840.
[160] Wang X, Gonzalez-Rodriguez D, Vourc'h T, Silberzan P and Abdul I. Barakat A I 2023 *Commun. Biol.* **6** 262
[161] Park J A, Youm Y, Lee H-R, Lee Y, Barron S L, Kwak T, Park G T, Song Y-C, Owens R M, Kim J H and Jung S 2023 *Adv. Mater.* **35** 2204390
[162] Wan X, Feng W, Wang Y, Wang H, Zhang X, Deng C and Yang N 2019 *Nano Lett.* **19** 3387
[163] Wang Z, Chen A, Tao K, Han Y and Li J 2024 *Adv. Mater.* **36** 2306733.
[164] Saito N, Nawachi A, Kondo Y, Choi J, Morimoto H and Ohshima T 2023 *Bull. Chem. Soc. Jpn.* **96** 465
[165] Nakaguro K, Mitsuta Y, Koseki S, Oshiyama T and Asada T 2023 *Bull. Chem. Soc. Jpn.* **96** 1099
[166] Kutsukake K 2024 *J. Crystal Growth* **630** 127598
[167] Chaikittisilp W, Yamauchi Y and Ariga K 2022 *Adv. Mater.* **34** 2107212.
[168] Oviedo L R, Oviedo V R, Martins M O, Fagan S B and da Silva W L 2022 *J. Nanopart. Res.* **24** 157